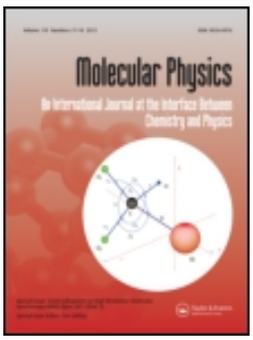

Taylor & Francis
Taylor & Francis Group

Molecular Physics

An International Journal at the Interface Between Chemistry and Physics

ISSN: 0026-8976 (Print) 1362-3028 (Online) Journal homepage: http://www.tandfonline.com/loi/tmph20

Multireference explicitly correlated F12 theories

Toru Shiozaki & Hans-Joachim Werner

To cite this article: Toru Shiozaki & Hans-Joachim Werner (2013) Multireference explicitly correlated F12 theories, Molecular Physics, 111:5, 607-630, DOI: 10.1080/00268976.2013.779393

To link to this article: http://dx.doi.org/10.1080/00268976.2013.779393

Accepted author version posted online: 22 Feb 2013.
Published online: 21 Mar 2013.

Molecular Physics, 2013
Vol. 111, No. 5, 607–630, http://dx.doi.org/10.1080/00268976.2013.779393

Taylor & Francis
Taylor & Francis Group

TOPICAL REVIEW

Multireference explicitly correlated F12 theories

Toru Shiozaki[†] and Hans-Joachim Werner[*]

Institut für Theoretische Chemie, Universität Stuttgart, Stuttgart, Germany

(*Received 4 December 2012; final version received 13 February 2013*)

We review our recent developments in multireference explicitly correlated F12 theories (explicitly correlated internally contracted multireference perturbation and multireference configuration interaction theories) that achieve near-basis-set-limit accuracy of the underlying multireference electron correlation methods with basis sets of medium size. The applicability of the multireference F12 theories is the same as that of their non-F12 counterpart, and therefore it is a computational tool with predictive accuracy for complicated electronic structures with strong correlation. A comparison with the earlier developments by others is also discussed.

Keywords: multireference methods; multireference configuration interaction; MRCI; multireference perturbation theory; CASPT2; explicit correlation; F12; internal contraction

1. Introduction

Even though the single-reference coupled-cluster (CC) hierarchy of methods [1] has been successful in achieving chemical accuracy or more for well-behaved systems [2], many important chemical processes undergo complicated electronic structures that demand multireference electron correlation theories. Such situations include many catalytic reactions with transition metal compounds, photorelaxation processes that go through conical intersections or low-spin, open-shell materials in spintronics. Many-electron excited states, such as the lowest states of long polyenes, retinal or carotene, are also often treated by multireference methods since the computation by standard single-reference methods involves unnecessarily large computational costs. However, since most theory developments in electronic structure theory have been devoted to single-reference theories, there is still a large gap between the sophistication of single-reference theories and that of multireference theories. In this paper, we review some recent developments that attempt to fill this gap.

The developments of multireference correlation methods in past decades have led to various well-established models. A complication arises through the fact that – in contrast to single-reference methods – the configuration space is not uniquely defined in the multireference case. Individual configuration state functions (CSFs) can be defined by specifying the occupation numbers for each spatial orbital (orbital configurations) and in addition the spin-coupling of the open-shell orbitals. The most straightforward way is to include in the wavefunction all single and double orbital excitations relative to each reference configuration and to take into account all possible spin-couplings for each orbital configuration. This leads to an expansion of CSFs whose number strongly increases with the number of reference configurations and open-shell orbitals. The coefficients (amplitudes) of the CSFs and the energy can be determined either variationally [multireference configuration interaction (MRCI)] [3] or by perturbation theory (multireference perturbation theory) [4–7].

Despite the fact that the Hamiltonian in a basis of CSFs is very sparse, the computational cost of standard MRCI very quickly increases with the number of reference configurations and electrons, and therefore the applicability of this method is limited. An alternative, which avoids this problem to a large extent, is to use contracted configuration expansions. Various contraction schemes have been proposed in the past. Probably most widely used are internally contracted configuration expansions [8, 9]. The internally contracted configurations are generated by applying excitation operators to the reference wavefunction as a whole. This means that the number of excited configurations becomes independent of the number of reference configurations; it only depends on the number of correlated orbitals, just as in single-reference theories. The internally contracted configurations exactly span the first-order interacting space of the reference function [8], and therefore the contraction has only a minor impact on the accuracy. As will be discussed in more detail later, it is also possible to mix contracted and uncontracted schemes.

Internally contracted [10] methods include the complete active space second-order perturbation method (CASPT2) [11–18] and N-electron valence state perturbation theory

[†]Present address: Department of Chemistry, Northwestern University, Evanston, IL 60208, USA; Email: shiozaki@northwestern.edu.
[*]Corresponding author. Email: werner@theochem.uni-stuttgart.de

(NEV-PT) [19–21], the internally contracted MRCI theory [10, 22–26], the canonical transformation theory [27–29], and the internally contracted multireference coupled-cluster theory (MRCC) [30, 31]. The applicability and efficiency of CASPT2 has recently been improved by combining CASPT2 with density fitting or Cholesky decomposition by Aquilante *et al.* [17, 32]. Recent developments in our group include a new internally contracted MRCI method for larger molecules by Shamasundar *et al.* [26], explicitly correlated CASPT2-F12 [33] and MRCI-F12 methods [34, 35] and the extended multistate CASPT2 method (XMS-CASPT2) of Shiozaki *et al.* [36, 37], which is based on Granovsky's work [38]. Analytical nuclear gradients for internally contracted CASPT2 were first implemented by Celani and Werner [39] and recently generalised to XMS-CASPT2 [36]. Analytical energy gradients for XMS-CASPT2 with density fitting have been implemented as well [40].

In the current work, we focus on our explicitly correlated multireference theories, namely CASPT2-F12 and MRCI-F12 [33–35]. The addition of -F12 to the denomination of a method means that terms that explicitly depend on the interelectronic distances r_{12} are included in the wavefunction. While early theories just used a linear r_{12} factor [41–43], most recent methods use an exponential function $F_{12}(r_{12}) = -\gamma^{-1}\exp(-\gamma r_{12})$ [44, 45]. These terms greatly improve the description of the wavefunction in the vicinity of electron–electron coalescence ($r_{ij} \to 0$) and therefore greatly improve the convergence of the energy with basis set size. Even though the F12 theory has been mainly developed in conjunction with the single-reference electronic structure methods, it is equally applicable to multireference theories since it is based on general physics encoded in the first quantised molecular Hamiltonian. An overview of our developments in MR-F12 theories will be presented with representative numerical results. Furthermore, a comparison will be made with related theories developed by others [46–52].

2. Internally contracted multireference electron correlation methods

We begin with a short introduction to internally contracted multireference electron correlation methods. In what follows, multiconfiguration self-consistent field (MCSCF) reference wavefunctions are used, which are a linear combination of reference CSFs ($|R\rangle$):

$$|0\rangle = \sum_R t_R^{(0)} |R\rangle. \tag{1}$$

Complete active space self-consistent field (CASSCF) type reference functions can be considered as a special case that is widely used. In this section, we will only consider electronic ground states. Excited state treatments will be summarised in the next section.

Table 1. Orbital spaces and associated indices used in this review. All orbitals are assumed to be orthonormal. The CABS space is orthogonal on all orbitals in the standard orbital basis set (OBS).

Space	Indices
Finite spaces:	
Occupied orbitals (including the core)	o, o'
Correlated (valence) orbitals	i, j, k, l, m, n
External orbitals in the OBS	a, b, c, d
All orbitals in the OBS	r, s, t, u
Complete (infinite) spaces:	
Any external orbitals	α, β
Any orbitals	κ, λ, μ, ν
CA orbitals	x, y

The orbitals that occur in any of the reference configurations are denoted by *occupied* or *internal* and labelled by indices i, j, k, l. The remaining *virtual* or *external* orbitals are labelled a, b, c, d. The occupied space can be further divided into *core* (not correlated), *valence* (correlated), *inactive* or *closed-shell* (doubly occupied in all reference CSFs), and *active* orbitals. The index notation is summarised in Table 1. In the following, we will distinguish *internal* configurations that have no electrons in the external orbital space, and singly and doubly external configurations with one or two electrons in the external orbitals, respectively.

We will employ spin-summed excitation operators

$$\hat{E}_s^u = \sum_{\sigma=\alpha,\beta} \eta_{u\sigma}^\dagger \eta_{s\sigma}, \tag{2}$$

$$\hat{E}_{rs}^{tu} = \sum_{\sigma=\alpha,\beta} \eta_{t\sigma}^\dagger \hat{E}_s^u \eta_{r\sigma}, \tag{3}$$

where $\eta_{r\sigma}^\dagger$ and $\eta_{s\sigma}$ are spin-orbital creation and annihilation operators for spin $\sigma = \{\alpha, \beta\}$. In general, internally contracted configurations are generated by applying these operators to the fixed reference function $|0\rangle$, e.g.

$$\Phi_i^r = \hat{E}_i^r |0\rangle, \tag{4}$$

$$\Phi_{ij}^{rs} = \hat{E}_{ij}^{rs} |0\rangle. \tag{5}$$

The internally contracted configurations are not orthogonal to each other and can be even linearly dependent. Their overlap and Hamiltonian matrix elements depend on the reduced density matrices (RDMs) of the reference function,

$$\gamma_{ij} = \langle 0|\hat{E}_j^i|0\rangle, \tag{6}$$

$$\Gamma_{ij,kl} = \langle 0|\hat{E}_{jl}^{ik}|0\rangle, \tag{7}$$

$$\Gamma_{ij,kl,mn} = \langle 0|\hat{E}_{jln}^{ikm}|0\rangle, \tag{8}$$

and so on. The highest order of the density matrix that is needed can be obtained by counting the occupied indices

that may be involved. For example, the overlap and Hamiltonian matrices of the internal double excitations Φ_{ij}^{kl} depend on the fourth- and sixth-order RDMs, respectively, while for the Hamiltonian matrix elements between doubly external configurations at most the second-order density matrix is needed. In the latter case, it is useful to define spin-coupled configurations

$$\left|\Phi_{ijp}^{ab}\right\rangle = \frac{1}{2}\left(\left|\Phi_{ij}^{ab}\right\rangle + p\left|\Phi_{ji}^{ab}\right\rangle\right) \quad (p = \pm 1), \tag{9}$$

where $p = 1$ and $p = -1$ denote singlet and triplet coupling, respectively, of the external electrons. The overlap matrix then factorises

$$\left\langle\Phi_{ijp}^{ab}\middle|\Phi_{klq}^{cd}\right\rangle = \frac{1}{2}(\delta_{ac}\delta_{bd} + p\delta_{ad}\delta_{bc})S_{ijp,klq}, \tag{10}$$

$$S_{ijp,klq} = \delta_{pq}\langle 0|\hat{E}_{kl}^{ij} + p\hat{E}_{lk}^{ij}|0\rangle, \tag{11}$$

and orthogonal configurations ($i \geq j$, $a \geq b$) can be obtained by diagonalising the internal overlap matrices $S_{ijp,\,klp}$ (separately for $p = 1$ and $p = -1$).

Fully internally contracted wavefunctions have been first investigated by Werner and Reinsch [10, 22, 23] and have been used later in various contexts [12, 13, 15, 17–19, 24, 25, 27–31]. The wavefunction is parametrised as

$$\left|\Psi^{\text{full}}\right\rangle = \sum_{ijp,kl} t_{kl}^{ijp}\left|\Phi_{ijp}^{kl}\right\rangle + \sum_{ijk,a} t_{ak}^{ij}\left|\Phi_{ij}^{ak}\right\rangle + \sum_{ijp,ab} t_{ab}^{ijp}\left|\Phi_{ijp}^{ab}\right\rangle. \tag{12}$$

For spin-coupled quantities, the summations are here and in the following implicitly restricted as $\sum_{ijp} \equiv \sum_{i\geq j}\sum_{p=\pm 1}$, and the amplitudes have the symmetry $t_{ab}^{ijp} = pt_{ba}^{ijp}$. The summations over external orbital labels a, b are always unrestricted. This implies

$$\frac{1}{2}\sum_{ij}\sum_{ab} t_{ab}^{ij}\left|\Phi_{ij}^{ab}\right\rangle = \sum_{ijp}\sum_{ab} t_{ab}^{ijp}\left|\Phi_{ijp}^{ab}\right\rangle. \tag{13}$$

In efficient computer codes, the occupied orbital space is divided into closed and active orbital spaces. All expressions can then be reduced so that all indices of the RDMs refer to active orbitals only. Nevertheless, the calculation and diagonalisation of high-order density matrices may become a bottleneck with large active spaces. Therefore, partially contracted wavefunction ansätze have been proposed in which the highest order of the required RDMs is reduced.

The first partially internally contracted wavefunction was developed by Werner and Knowles (WK) [24, 25]. They used the ansatz

$$\left|\Psi^{\text{WK}}\right\rangle = \sum_{I} t_I\left|I\right\rangle + \sum_{S,a} t_a^S\left|S^a\right\rangle + \sum_{ijp,ab} t_{ab}^{ijp}\left|\Phi_{ijp}^{ab}\right\rangle, \tag{14}$$

where only the doubly external space internally contracted, while the standard CSFs $|I\rangle$ and $|S^a\rangle$ are used for the internal and singly external CSFs, respectively. The N-electron CSFs $|I\rangle$ are obtained by generating all orbital configurations that differ by at most two electrons from any reference configuration, and then associating all possible spin-couplings to each orbital product. Note that this space includes all reference configurations ($\{R\}\subseteq\{I\}$), and the coefficients of the reference CSFs are therefore fully relaxed in the MRCI (but not in CASPT2, see below). Similarly, the $N-1$ electron functions S are generated by two electron annihilations and one creation, and again all spin-couplings are included (the external electron in orbital a is coupled last). For further details, we refer to Refs. [24, 25].

A more sophisticated partial internal contraction scheme has been proposed by Celani and Werner (CW) [16]. In this case, the internal contraction is used for all configuration subspaces whose overlap matrix is described by just the one- and two-particle active-space RDMs (1RDM and 2RDM, respectively). The occupied orbital space is divided into two spaces: the closed orbital (labelled by i_c, j_c) and active orbital spaces (i_a, j_a). The CW contracted wavefunction is defined as

$$\begin{aligned}\left|\Psi^{\text{CW}}\right\rangle = &\sum_{I_0} t_{I_0}\left|I_0\right\rangle + \sum_{I_1} t_{I_1}\left|I_1\right\rangle + \sum_{i_cj_cp,i_aj_a} t_{i_aj_a}^{i_cj_cp}\left|\Phi_{i_cj_cp}^{i_aj_a}\right\rangle \\ &+ \sum_{S_0,a} t_a^{S_0}\left|S_0^a\right\rangle + \sum_{i_c,i_aj_a,a} t_{aj_a}^{i_ci_a}\left|\Phi_{i_ci_a}^{aj_a}\right\rangle \\ &+ \sum_{i_c,i_aj_a,a} t_{aj_a}^{i_ai_c}\left|\Phi_{i_ai_c}^{aj_a}\right\rangle + \sum_{i_cj_c,i_a,a} t_{ai_a}^{i_cj_c}\left|\Phi_{i_cj_c}^{ai_a}\right\rangle \\ &+ \sum_{ijp,ab} t_{ab}^{ijp}\left|\Phi_{ijp}^{ab}\right\rangle,\end{aligned} \tag{15}$$

where subscripts on CSFs denote the number of holes in the closed orbital space. Here only the spaces I_0, I_1 and S_0 are left uncontracted, since these are the only ones that depend on more than two active orbital labels. This ansatz was first used for CASPT2 [16] and has very recently been extended to MRCI [26]. Since, on the one hand, the number of uncontracted CSFs is strongly reduced and, on the other hand, all RDMs and coupling coefficients depend on active orbital labels only, these methods are much more efficient than their older counterparts that used the WK scheme. However, the explicit expressions for MRCI are extremely lengthy and could only be derived and implemented using automated techniques [26, 53].

Given the parametrisation of the wavefunction, one minimises the Hylleraas functional,

$$E_2 = \langle \Psi^{(1)} | \hat{H}^{(0)} - E_0 | \Psi^{(1)} \rangle + 2 \langle \Psi^{(1)} | H | 0 \rangle, \quad (16)$$

with respect to all t amplitudes in the wavefunction to arrive at the CASPT2 method, or the energy expectation value,

$$E = \frac{\langle \Psi | H | \Psi \rangle}{\langle \Psi | \Psi \rangle}, \quad (17)$$

to define the MRCI method. For example, in the WK-MRCI case this leads to the CI eigenvalue equation

$$r_I = \langle I | \hat{H} - E | \Psi^{\mathrm{WK}} \rangle = 0, \quad (18)$$

$$r_a^S = \langle S^a | \hat{H} - E | \Psi^{\mathrm{WK}} \rangle = 0, \quad (19)$$

$$r_{ab}^{ijp} = \langle \Phi_{ijp}^{ab} | \hat{H} - E | \Psi^{\mathrm{WK}} \rangle = 0. \quad (20)$$

These coupled equations can be solved iteratively (direct CI) by computing in each iteration the *residuals* r_I, r_a^S and R_{ab}^{ijp}, and using these to obtain perturbative updates of the amplitudes, e.g.

$$\Delta t_I = \frac{-r_I}{\langle I | \hat{H} - E | I \rangle}, \quad (21)$$

$$\Delta t_a^S = \frac{-r_a^S}{\langle S^a | \hat{H} - E | S^a \rangle}. \quad (22)$$

A slight compilation arises for the doubly external excitations, since the internally contracted basis is not orthogonal. In order to avoid convergence problems due to the non-orthogonality, it is necessary to transform to an orthonormal basis $|\Phi_{Dp}^{ab}\rangle$, which is related to the non-orthogonal ones by the linear transformation

$$|\Phi_{Dp}^{ab}\rangle = \sum_{i \le j} T_D^{ijp} |\Phi_{ijp}^{ab}\rangle, \quad (23)$$

where T_D^{ijp} is the inverse of the square root of $S_{ijp,\,klp}$ [cf. Equation 11]. Correspondingly, the residuals for the doubly external configurations are transformed into the orthogonal basis

$$R_{ab}^{Dp} = \sum_{i \le j} T_D^{ijp} r_{ab}^{ijp}, \quad (24)$$

and the amplitudes are then updated in this basis:

$$\Delta t_{ab}^{Dp} = \frac{-R_{ab}^{Dp}}{\langle \Phi_{Dp}^{ab} | \hat{H} - E | \Phi_{Dp}^{ab} \rangle}. \quad (25)$$

The denominators can be approximated as described in Ref. [22]. Finally, the amplitudes are transformed back to the non-orthogonal one

$$\Delta t_{ab}^{ijp} = \sum_D T_D^{ijp} \Delta t_{ab}^{Dp}. \quad (26)$$

Internally contracted internal and singly external configurations, as used in the CW contraction scheme, can be treated in an analogous way [16, 26]. A modified Davidson procedure as described in Ref. [24] is used to guarantee and speed up convergence.

In summary, the internal contraction reduces the number of amplitudes while increasing the rank of the RDMs needed to evaluate the overlap and residual vectors. The CW internal contraction is perhaps the best compromise for most cases. However, due to the complicated structure of the explicit expressions resulting in the CW scheme, we have still used the WK internal contraction in the development of our CASPT2-F12 and MRCI-F12 methods. The extension to the CW scheme will be developed in the future.

3. Internally contracted wavefunctions for excited states

The internally contracted configuration spaces defined above are state-specific, since they are created from a given reference state $|0\rangle$. In order to compute electronically excited states, there are various choices: the first possibility is to calculate each state separately, using the appropriate reference function for each state. This works well in cases where the states are energetically well separated and the states under consideration do not strongly mix. Such single-state (SS) internally contracted functions are often used in CASPT2. Since in the first-order CASPT2 wavefunction the reference function is not relaxed (i.e. the coefficients of the reference CSFs do not change), the optimisation of the amplitudes for excited states is no problem. However, in MRCI it is much more difficult to converge to a specific root since the coefficients of the reference configurations may change and root-flipping problems can occur.

The internally contracted SS treatment fails entirely if states become nearly degenerate and strongly mix in the CASPT2 or MRCI wavefunctions. A partial remedy is provided by the MS-CASPT2 method proposed by Finley *et al.* [15], in which at the end of the calculation an approximate second-order effective Hamiltonian is constructed in the basis of the SS wavefunctions and diagonalised. In the case of MRCI, a projection method has been proposed [54] in which one state after the other is computed, and in each case the internal parts of the previous wavefunctions are projected out. Each excited state calculation then proceeds like a ground-state one and no convergence problems occur any more. Similar to the MS-CASPT2 case, at the end the Hamiltonian and overlap matrices are constructed in the (non-orthogonal) basis of the SS wavefunctions and the

corresponding eigenvalue problem is solved in order to get orthogonal states and variational energies.

The most accurate approach to treat excited states is to generate the internally contracted configurations from all reference states under consideration, and then use the union of all these to expand the wavefunctions of all states [54]. This basis is invariant with respect to rotations among the reference functions and is therefore suitable to treat narrow avoided crossings or conical intersections. In the MRCI, all states can then be optimised simultaneously and orthogonal eigenstates are obtained. A disadvantage of this method is, however, that the computational effort increases almost quadratically with the number of states. The MS basis can also be used in MS-CASPT2 (as implemented in MOLPRO). However, artefacts on the potential energy surfaces (PESs) can still occur near conical intersections. This problem can be solved by using a zeroth-order Hamiltonian that is also invariant to unitary transformations of the reference functions, as first proposed by Granovsky [38] for uncontracted wavefunctions and extended by us to internally contracted MS-CASPT2 [36, 40]. Using the resulting so-called XMS-CASPT2 method perfectly smooth PESs are obtained even near conical intersections [55].

4. Background of explicitly correlated F12 theories

In this section, we briefly review the single-reference F12 theories. Interested readers should refer to, for instance, the reviews in Refs. [56–59], and references therein, for more details.

In the complete basis set (CBS) limit, an electronic wavefunction of N electrons is a vector in the antisymmetrised part of the $3N$-dimensional Hilbert space, where antisymmetrisation is the reflection of the Pauli exclusion principle. Practically, however, the molecular Schrödinger equation needs to be cast onto a finite problem and to be solved numerically, since the first quantised Schrödinger equation has no analytic solutions in a closed form except for a few simplest cases. In conventional (non-F12) theories, this is done by introducing a so-called one-electron basis set, and expressing the wavefunction in terms of antisymmetrised products of spin-orbitals (Slater determinants).

However, molecular electronic wavefunctions represented by products of one-electron basis functions have been known to converge only slowly with respect to basis size towards the CBS limit, as already pointed out by Hylleraas in 1929 [60]. The slow convergence is attributed to the poor description of the electron–electron cusps at electron coalescence ($r_{12} = 0$) and the electronic structure around them. According to Kato's condition [61] and its refinement by Pack and Byers Brown [62], the first-order wavefunctions for two electrons have the cusps of the form

$$\Phi^{(1)}_{m=0} = \left(1 + \tfrac{1}{2} r_{12}\right) \Phi^{(0)}(r_{12} = 0) + O\left(r_{12}^2\right), \quad (27)$$

$$\Phi^{(1)}_{m=1} = \left(1 + \tfrac{1}{4} r_{12}\right) \mathbf{r}_{12} \cdot \frac{\partial \Phi^{(0)}}{\partial \mathbf{r}_{12}} + O(r_{12}^3), \quad (28)$$

where $\Phi^{(1)}_{m=0}$ and $\Phi^{(1)}_{m=1}$ are the singlet and triplet coupled first-order wavefunctions, whereas $\Phi^{(0)}$ is the corresponding Hartree–Fock (HF) determinant. $r_{12} = |\mathbf{r}_1 - \mathbf{r}_2|$ is the distance between the two electrons. These conditions cannot be fulfilled by a finite expansion in terms of Slater determinants. Back in the 1920s, Hylleraas already proposed to represent the wavefunctions of two-electron atoms as

$$\Psi = e^{-\zeta(r_1 + r_2)} \sum_{lmn} C_{lmn} (r_1 + r_2)^l (r_1 - r_2)^m r_{12}^n, \quad (29)$$

which directly span the six-dimensional Hilbert space for totally symmetric wavefunctions. The convergence of total energies with respect to basis size has been shown to be much faster than the conventional CI expansions [60]. Since then, there have been many studies along this line, including the 'transcorrelated' [63–65] and Gaussian-type geminal methods [66–68] to name a few, which have been nonetheless limited to very small systems. For detailed accounts on earlier works, refer to other reviews [69, 70].

A major breakthrough was brought by the seminal work of Kutzelnigg in 1985 [41], in which he has proposed the so-called R12 method that uses two-electron basis functions to augment the conventional determinant-based wavefunction expansions. In the R12 method, a two-electron wavefunction was parametrised as

$$|\Psi\rangle = (1 + t\hat{Q}_{12} r_{12}) \Phi_{\mathrm{HF}} + \sum_{ab} t_{ab} \Phi_{ab}, \quad (30)$$

$$\hat{Q}_{12} = \sum_{\alpha\beta} |\alpha\beta\rangle\langle\alpha\beta|, \quad (31)$$

where Φ_{HF} and Φ_{ab} are the reference and excited Slater determinants, respectively, and t and t_{ab} are the parameters to be optimised. $\hat{Q}_{12}$ is a strong orthogonality projector that keeps the r_{12}-dependent term orthogonal to the reference function and singly excited Slater determinants. Here α and β label virtual orbitals in the complete basis whose size is infinite (cf. Table 1). The essential difference between the R12 and earlier methods lies in the fact that the R12 method introduces the geminal factor as a (normally small) correction to the conventional wavefunction. The projection makes the geminal excitation commutable with the conventional excitations, thereby making it possible to include them in conventional electron correlation methods.

In the following years, this ansatz was generalised for many-electron systems by Klopper and Kutzelnigg and first implemented for the Møller–Plesset perturbation theory (MP2-R12) [42, 43, 71]. We restrict the following discussion to the closed-shell case in a real spin-free formulation that does not follow exactly the original formulation of

Klopper and Kutzelnigg. Throughout this paper, the two-electron bras and kets are simple orbital products, e.g. $|ij\rangle = \phi_i(\mathbf{r}_1)\phi_j(\mathbf{r}_2)$, and the integrals over two-electron operators $\hat{O}_{12}$ are defined as

$$\langle\alpha\beta|\hat{O}_{12}|ij\rangle = \int_{\mathcal{R}_3} d\mathbf{r}_1 \int_{\mathcal{R}_3} d\mathbf{r}_2\ \phi_\alpha(\mathbf{r}_1)\phi_\beta(\mathbf{r}_2) \times \hat{O}_{12}\phi_i(\mathbf{r}_1)\phi_j(\mathbf{r}_2). \quad (32)$$

In the orbital invariant ansatz of Klopper [71], the MP2-R12 first-order wavefunction is parametrised as

$$\left|\Psi^{(1)}\right\rangle = \frac{1}{2}\sum_{ij}\left[\sum_{ab} t_{ab}^{ij}\left|\Phi_{ij}^{ab}\right\rangle + \sum_{kl} t_{kl}^{ij}\left|\Phi_{kl}^{ij}\right\rangle\right], \quad (33)$$

$$\left|\Phi_{ij}^{kl}\right\rangle = \sum_{\alpha\beta}\left|\Phi_{ij}^{\alpha\beta}\right\rangle\left\langle\alpha\beta\left|\hat{Q}_{12}r_{12}\right|kl\right\rangle, \quad (34)$$

$$\hat{Q}_{12} = (1-\hat{o}_1)(1-\hat{o}_2) - \hat{v}_1\hat{v}_2. \quad (35)$$

The parameters ('amplitudes') t_{kl}^{ij} and t_{ab}^{ij} can be optimised by minimising the Hylleraas functional [cf. Equation 16]. The minimum of E_2 with respect to the amplitudes equals the second-order MP2-R12 energy $E^{(2)}$.

The first summation in the square brackets of Equation (33) corresponds to the conventional double excitations from occupied orbitals i, j into virtual orbitals a, b, as present in any MP2 wavefunction. The second summation involves in addition explicitly correlated configurations Φ_{ij}^{kl}, which can be viewed as an "external contraction" of an infinite set of double excitations $\Phi_{ij}^{\alpha\beta}$ with contraction coefficients $\langle\alpha\beta|\hat{Q}_{12}r_{12}|kl\rangle$. The summation in Equation (34) over the infinite number of virtual orbitals (α and β) is just a mathematical device and avoided in the actual working equations by new analytical integrals (see further below).

The strong orthogonality projector $\hat{Q}_{12}$ defined in Equation (35) makes the explicitly correlated part in the wavefunction strongly orthogonal to the conventional MP2 wavefunction. $\hat{o}_1$ and $\hat{o}_2$ are one-electron projectors onto the occupied orbital space, i.e. $\hat{o}_i = \sum_o |\phi_o(\mathbf{r}_i)\rangle\langle\phi_o(\mathbf{r}_i)|$. Similarly, the operators $\hat{v}_i = \sum_a |\phi_a(\mathbf{r}_i)\rangle\langle\phi_a(\mathbf{r}_i)|$ project onto the virtual space. The last term in the projector ensures that $\langle ab|\hat{Q}_{12}r_{12}|kl\rangle = 0$, i.e. there are no contributions of the conventional double excitations in Equation (34). The terms involving $\hat{o}_1$ and $\hat{o}_2$ further ensure that all terms vanish in which α or β correspond to an occupied orbital. One can therefore replace the double sum over the complete *virtual* space by a double sum over the *full* space. In the explicit expressions of the Hamiltonian matrix elements, this leads to exact resolutions of the identity, which make it possible to remove these summations entirely. For example, the Hylleraas functional contains terms such as

$$\langle\Phi_{\mathrm{HF}}|\hat{H}|\Phi_{ij}^{kl}\rangle = \sum_{\mu,\nu}\langle\Phi_{\mathrm{HF}}|\hat{H}|\Phi_{ij}^{\mu\nu}\rangle\langle\mu\nu|\hat{Q}_{12}r_{12}|kl\rangle$$
$$= \sum_{\mu,\nu}[2\langle ij|r_{12}^{-1}|\mu\nu\rangle - \langle ji|r_{12}^{-1}|\mu\nu\rangle]\langle\mu\nu|\hat{Q}_{12}r_{12}|kl\rangle$$
$$= 2\langle ij|r_{12}^{-1}\hat{Q}_{12}r_{12}|kl\rangle - \langle ji|r_{12}^{-1}\hat{Q}_{12}r_{12}|kl\rangle. \quad (36)$$

The difficulty now is that the terms $\hat{o}_1 + \hat{o}_2$ in the projector lead to three- and four-electron integrals, e.g.

$$\left\langle ij\left|r_{12}^{-1}\hat{o}_1 r_{12}\right|kl\right\rangle = \textstyle\sum_o \left\langle ijo\left|r_{12}^{-1}r_{23}\right|olk\right\rangle. \quad (37)$$

Kutzelnigg proposed to avoid these integrals by approximate resolutions of the identity [41–43]. By inserting identity operators $u_i = \sum_\kappa |\kappa(i)\rangle\langle\kappa(i)|$ the strong-orthogonality projector can be rewritten as

$$\hat{Q}_{12} = 1 - (\hat{o}_1\hat{u}_2 + \hat{u}_1\hat{o}_2) + \hat{o}_1\hat{o}_2 - \hat{v}_1\hat{v}_2$$
$$= 1 - \sum_o\sum_\kappa(|o\kappa\rangle\langle o\kappa| + |\kappa o\rangle\langle\kappa o|) + \sum_{o,o'}|oo'\rangle\langle oo'| - \sum_{a,b}|ab\rangle\langle ab|. \quad (38)$$

The three-electron integrals then factorise into sums of products of two-electron integrals:

$$\langle ij|r_{12}^{-1}\hat{o}_1 r_{12}|kl\rangle = \delta_{ik}\delta_{jl} - \sum_{o,\kappa}\left(\langle ij|r_{12}^{-1}|o\kappa\rangle\langle o\kappa|r_{12}|kl\rangle + \langle ij|r_{12}^{-1}|\kappa o\rangle\langle\kappa o|r_{12}|kl\rangle\right) + \sum_{o,o'}\langle ij|r_{12}^{-1}|oo'\rangle\langle oo'|r_{12}|kl\rangle - \sum_{a,b}\langle ij|r_{12}^{-1}|ab\rangle\langle ab|r_{12}|kl\rangle \quad (39)$$

This expression is exact if the summation over κ runs over a complete orthonormal basis of one-electron orbitals. In the resolution of the identity (RI) approximation, this is replaced by a finite basis (RI basis).

In the early R12 methods, the RI basis was taken equal to the orbital basis ('Standard Approximation'). The projector in Equation (38) then reduces to

$$\hat{Q}_{12} = 1 - \sum_{r,s}|rs\rangle\langle rs| \quad (40)$$

and all integrals can be expressed in the orbital basis. Furthermore, the equations for the amplitudes of the conventional and explicitly correlated terms decouple and can be solved independently.

Subsequently, the R12 method was generalised to CI and CC theories [72, 73] as well as to multireference methods [46, 47]. The problem with all these approaches was, however, that a very large orbital basis had to be used in order to get a sufficiently accurate representation of the RIs in the standard approximation. Therefore, these methods could be applied only for benchmark calculations on atoms and very small molecules.

On the basis of these pioneering works, there has been an explosion of theoretical developments in the 2000s leading to sophisticated implementations [74–77]. This started with the introduction of auxiliary basis functions for the RI, first by Klopper and Samson [78], and later refined by Valeev [79] [the so-called complementary auxiliary basis set (CABS) scheme]. In the CABS approach, the one-electron unit operators are expressed by the union of the orbital basis (denoted by indices r, s) and a CA basis (denoted by indices x, y), which is orthogonal to the orbital basis, i.e. $\langle r|s\rangle = \delta_{rs}$, $\langle x|y\rangle = \delta_{xy}$, $\langle x|r\rangle = 0$ for all r, s, x, y. Using Equations (35) and (38) this leads to

$$\hat{u}_i = \sum_r |r(i)\rangle\langle r(i)| + \sum_x |x(i)\rangle\langle x(i)|, \tag{41}$$

$$\hat{Q}_{12} = 1 - \sum_{r,s} |rs\rangle\langle rs| - \sum_{x,o} \left(|xo\rangle\langle xo| + |ox\rangle\langle ox| \right). \tag{42}$$

The main advantage of the CABS approach is that various contributions in the orbital basis cancel, and this leads to simplifications in the equations, in particular in explicitly correlated CC methods. Furthermore, the last summation in Equation (42) that involves the CA orbitals x is usually a small correction and can be neglected in some coupling terms without significant loss of accuracy.

The hope was that accurate results could be obtained by using small orbital basis sets along with larger RI or CABS basis sets. It turned out, however, that the accuracy of the MP2-R12 method was still unsatisfactory, unless large orbital basis sets were used. The reason is that the linear r_{12} correlation factor is only reasonable for small r_{12}, but unphysical at large values of r_{12}. A large basis set is then needed to compensate for this qualitatively wrong behaviour, and serious numerical problems can occur in larger molecules. These problems were cured by Ten-no [44, 45], who proposed to replace the linear correlation factor r_{12} in Equation (34) by a Slater-type geminal function

$$F_{12}(r_{12}) = -\gamma^{-1} e^{-\gamma r_{12}} = -\gamma^{-1} + r_{12} - \frac{1}{2}\gamma r_{12}^2 + \cdots \tag{43}$$

It was shown in numerous benchmarks that this leads to a dramatic improvement of the accuracy and numerical stability. Note that the first-order cusp conditions can still be satisfied using this function, since due to the strong-orthogonality projector the first term $(-\gamma^{-1})$ in the Taylor expansion of the exponential gives no contribution in Equation (34). Furthermore, Ten-no showed that the amplitudes t_{kl}^{ij} can be determined from the first-order cusp conditions. This yields

$$t_{kl}^{ij} = \frac{3}{8}\delta_{ik}\delta_{jl} + \frac{1}{8}\delta_{il}\delta_{jk}. \tag{44}$$

This so-called SP or FIX ansatz avoids the need to solve any equations for the amplitudes t_{kl}^{ij}. Nevertheless, it gives often more accurate relative energies than the full optimisation of all t_{kl}^{ij}. This is due to the fact that so-called geminal superposition errors are avoided [80, 81]. These errors can also be avoided by just optimising the amplitudes t_{ij}^{ij} and t_{ji}^{ij} and setting all remaining ones to zero (*diagonal* ansatz) [78, 81]. In contrast to the FIX ansatz, the *diagonal* ansatz is not orbital-invariant and only size-consistent if localised orbitals are used. However, it is advantageous in cases where the core–valence correlation is important [82].

Further improvements were density fitting for the F12 integrals [83, 84], efficient ways to compute intermediate quantities [81, 85], CABS singles corrections [86–89] that reduce the error of the underlying HF energies, and automated implementation schemes [90–93]. Recently the F12 theory has been extended to local correlation theories [94–98], theories with periodic boundary conditions [99], relativistic theories [100–104], response properties [105–109], and high-rank connected excitations [110, 111]. Of most practical importance was probably the development of accurate and efficient approximate CC-F12 models (such as CCSD(T)(F12) [112–114], CCSD(T)-F12x [86, 87, 115], CCSD(T)$_{\mathrm{F12}}$ [116–118], and CCSD(T)(F12*) [119]), which can now be routinely used in computational chemistry. It is generally accepted that the F12 methods yield with triple-ζ basis sets results that are at least as accurate as conventional calculations with quintuple-ζ basis sets. In the CCSD(T)-F12x methods [86, 87, 115] developed in our group, the extra effort for the F12 contributions only scales as $\mathcal{O}(N^5)$, where N is a measure of the molecular size. Since CCSD(T) calculations scale as $\mathcal{O}(N^7)$, the extra effort for the F12 treatment is very small in larger molecules, and therefore the F12 terms should always be included. The scaling can be further reduced by local approximations with hardly any loss of accuracy [96, 98]. Using such LCCSD(T)-F12 methods it is currently possible to carry out highly accurate calculations for molecules with more than 50 atoms. A new massively parallel linear-scaling implementation of closed-shell and open-shell LCCSD(T)-F12 methods, which will allow calculations on even much larger molecules, is currently in progress in our group.

5. Earlier multireference R12/F12 theories

In this section, some earlier multireference R12/F12 theories are reviewed with emphasis on the relation with our methods that will be presented in the subsequent sections. The main difference lies in how we define the *excitation part* of the geminal function with respect to the multideterminant reference function.

In the early 1990s, Gdanitz was the first to combine the R12 and multireference theories [46, 47], in which the excitation part of the geminal function (a linear factor $F_{12}(r_{12})$

$= r_{12}$ back then) with respect to each determinant $|I\rangle$ in the reference space was included. The wavefunction was parametrised as

$$|\Psi\rangle = |\Psi_{\rm conv}\rangle + \frac{1}{2}\sum_{I\in R}\sum_{ijkl} t^{ij}_{kl,I}\sum_{\alpha\beta}\langle\alpha\beta|\hat{Q}^I_{12}r_{12}|kl\rangle\hat{E}^{\alpha\beta}_{ij}|I\rangle, \tag{45}$$

where i, j in this equation are the occupied orbitals in each $|I\rangle$, and α and β are the corresponding virtual (unoccupied) orbitals for the same $|I\rangle$. $\hat{Q}^I_{12}$ projects out the contributions of conventional excitations arising from the reference configuration $|I\rangle$. The implementation of Gdanitz has been based on the Standard Approximation that employs the orbital basis functions for the RI, and therefore has been limited to application for small systems with a large basis set. In addition, since the geminal excitations become quickly linearly dependent, one had to omit some unimportant configurations in the reference space. The very recent extension of the F12 method to the Brillouin–Wigner MRCC method by Kedžuch *et al.* [50] can be seen as a generalisation of Gdanitz's work, though they have adopted the FIX ansatz.

For the following discussion it is useful to define the geminal excitation operator

$$\hat{F} = \frac{1}{2}\sum_{ij}\sum_{\alpha\beta}\mathcal{F}^{ij}_{\alpha\beta}\hat{E}^{\alpha\beta}_{ij} + \sum_{ij}\sum_{\alpha k}\mathcal{F}^{ij}_{\alpha k}\hat{E}^{\alpha k}_{ij}, \tag{46}$$

$$\mathcal{F}^{ij}_{\mu\nu} = \sum_{kl}\langle\mu\nu|F_{12}(r_{12})|kl\rangle t^{ij}_{kl}, \tag{47}$$

as well as the strong-orthogonality projectors $\hat{Q}_S$ and $\hat{Q}_P$ that project onto the doubly excited configurations with one or two electrons in the external orbital space, respectively, that are not contained in the conventional wavefunction. The projector $\hat{Q}_P$ can be written as

$$\hat{Q}_P = \sum_{Dp}\left[\sum_{xy}|\Phi^{xy}_{Dp}\rangle\langle\Phi^{xy}_{Dp}| + \sum_{ax}|\Phi^{ax}_{Dp}\rangle\langle\Phi^{ax}_{Dp}| + |\Phi^{xa}_{Dp}\rangle\langle\Phi^{xa}_{Dp}|\right], \tag{48}$$

where $|\Phi^{\alpha\beta}_{Dp}\rangle$ is a complete set of orthonormal internally contracted doubly external configurations as defined in Equation (23). This implies

$$\hat{Q}_P\hat{F} = \frac{1}{2}\sum_{ij}\sum_{\alpha\beta}\mathcal{T}^{ij}_{\alpha\beta}\hat{E}^{\alpha\beta}_{ij} = \sum_{ijp}\sum_{\alpha\beta}\mathcal{T}^{ijp}_{\alpha\beta}\hat{E}^{\alpha\beta}_{ijp}, \tag{49}$$

$$\mathcal{T}^{ij}_{\alpha\beta} = \sum_{kl}\langle\alpha\beta|\hat{Q}_{12}F_{12}|kl\rangle t^{ij}_{kl}, \tag{50}$$

$$\mathcal{T}^{ijp}_{\alpha\beta} = \frac{1}{2}\left(\mathcal{T}^{ij}_{\alpha\beta} + p\mathcal{T}^{ji}_{\alpha\beta}\right), \tag{51}$$

where $\hat{Q}_{12}$ is the two-electron projector as defined in Equations (35) and (42). If the FIX ansatz [Equation 44] is used, the quantities $\mathcal{T}^{ijp}_{\alpha\beta}$ simplify to

$$\mathcal{T}^{ijp}_{\alpha\beta} = \frac{1}{2}t_{ijp}\left(\bar{F}^{ij}_{\alpha\beta} + p\bar{F}^{ji}_{\alpha\beta}\right), \tag{52}$$

$$\bar{F}^{ij}_{\alpha\beta} = \langle\alpha\beta|\hat{Q}_{12}F_{12}|ij\rangle, \tag{53}$$

where t_{ijp} is $1/(2 + 2\delta_{ij})$ and $1/4$ for $p = 1$ and $p = -1$, respectively.

In 2007, Ten-no has reported the MRMP-F12 method [48], which used most of the modern F12 techniques mentioned in Section 4. In addition, his implementation has introduced internally contracted geminal excitations (though the underlying MRMP was uncontracted) of the form

$$|\Psi\rangle = |\Psi_{\rm conv}\rangle + \hat{Q}_P\hat{F}|0\rangle. \tag{54}$$

The FIX ansatz (cf. Equation 44) has been used for the geminal amplitudes t^{ij}_{kl}. Note that semi-internal geminal excitations arising from the second part of the operator $\hat{F}$ (cf. Equation 46) are not included in his theory. Besides the formal ansatz, Ten-no has simplified the formula by the extended Brillouin condition and the so-called Approximation A, making the F12 correction additive without the need of active 3RDMs. The work of Varganov and Martínez [120] is also related to Ten-no's work, though they omit the conventional excitation from the wavefunction and optimise orbitals self-consistently.

More recently, Valeev and coworkers have proposed a unique a posteriori correction to arbitrary wavefunction models [49, 51]. The theory is based on the extended normal ordering of Kutzelnigg and Mukherjee [121] to extract the excitation part of the geminal function with respect to the correlated wavefunction of the underlying dynamic correlation model. By neglecting high-order cumulants, they arrive at a formula expressed by contractions of the full correlated 2RDM and geminal tensors. Therefore, it is applicable to any method that provides 2RDMs for the full correlated N-electron wavefunction, even when wavefunctions are not well defined (e.g. determinant-based quantum Monte Carlo [122, 123]). In their original formulation [49], this universality has nonetheless demanded multiple $n^6_{\rm bas}$ operations where $n_{\rm bas}$ is the number of one-electron basis functions. As will be shown in the following sections, our MRCI-F12 method does not involve the RDMs in the full orbital basis but only *active-space* RDMs, which are the same as in the underlying MRCI method. It should be noted, however, that Valeev and coworkers have also studied an alternative formulation of their perturbative scheme to reduce the computational cost [51].

6. The MR-F12 wavefunction ansatz

We now turn to the CASPT2-F12 and MRCI-F12 methods developed by us [33–35]. Since both these methods have only linear excitations, their wavefunctions are parametrised in exactly the same way; only the expansion coefficients are determined differently. The MR-F12 wavefunctions of our studies are based on the WK internal contraction and read as follows [33]:

$$|\Psi\rangle = |\Psi^{\mathrm{WK}}\rangle + t_{\mathrm{F12}}\hat{Q}\hat{F}|0\rangle, \tag{55}$$

where $\hat{F}$ is defined in Equation (46), $\hat{Q} = \hat{Q}_S + \hat{Q}_P$, and $|\Psi^{\mathrm{WK}}\rangle$ constitute the conventional WK contracted wavefunction (cf. Equation 14). An extension to the more efficient CW contraction scheme (cf. Section 2) is straightforward though cumbersome and will be done in the future using automated techniques. The term $\hat{Q}\hat{F}|0\rangle$ in Equation (55) represents the internally contracted F12 double excitations. This ansatz is similar to the one by Ten-no [48] (cf. Equation 54) but includes in addition the semi-internal part of the geminal excitations, as in the perturbative correction of Torheyden and Valeev [49].

The geminal part of the wavefunction can be scaled by the additional parameter t_{F12}. Using in Equation (47) the fixed amplitudes (Equation 44), the first-order cusp conditions are fulfilled with

$$t_{\mathrm{F12}} = \frac{1}{c_0}, \tag{56}$$

$$c_0 = \langle 0|\Psi\rangle, \tag{57}$$

i.e. $t_{12} = 1$ in intermediate normalisation. In the MRCI case, it is also possible to optimise t_{12} variationally (cf. Section 7.2).

The operator $\hat{Q}_S$ projects onto the CSFs with one electron in CABS orbitals x:

$$\hat{Q}_S = \sum_{S,x} |S^x\rangle\langle S^x| \left[1 - \sum_{mn} |\Phi_m^x\rangle(\boldsymbol{\gamma}^{-1})_{mn}\langle\Phi_n^x|\right]. \tag{58}$$

The last term projects out internally contracted single excitations $|\Phi_m^x\rangle = \hat{E}_m^x|0\rangle$, as in Ref. [49], in order to assure that only the two-body part of the geminal excitations is used in the theory. The inverse of the 1RDM appears in Equation (58) since the internally contracted single configurations are in general not orthogonal to each other, i.e. $\langle\Phi_m^x|\Phi_n^y\rangle = \delta_{xy}\gamma_{mn}$ (they are only orthonormal if natural active orbitals are used). Rather than using all excitations into the full (infinite) CABS space, we approximate the semi-internal geminal excitations in the finite space of configurations $|S^x\rangle$. The energies based on this approximation have been proven to converge quickly with the size of the CABS space, both theoretically and numerically [48, 33]. The singles geminal part can now be written as

$$\hat{Q}_S\hat{F}|0\rangle = \sum_{S,x} |S^x\rangle\mathcal{F}_x^S \tag{59}$$

with

$$\mathcal{F}_x^S = \sum_T \left(\delta_{ST} - \sum_m D_m^S D_m^T\right) \sum_{ijk} \langle T^x|\hat{E}_{ij}^{xk}|0\rangle\mathcal{F}_{xk}^{ij}, \tag{60}$$

$$D_m^S = \sum_n \langle S^x|\hat{E}_n^x|0\rangle(\boldsymbol{\gamma}^{-1/2})_{mn}. \tag{61}$$

In our earlier implementation [33], we have used extended normal ordering [121] to extract the two-body part of the geminal excitations, instead of projecting out singles contributions as described above. The projection by normal ordering is weaker in a sense that the normal-ordered, two-electron excitations have non-zero overlap with the normal-ordered one-electron excitations as

$$\langle 0|\{\hat{E}_a^i\}\{\hat{E}_{jl}^{ak}\}|0\rangle = \Gamma_{ij,kl} - \gamma_{ij}\gamma_{kl} + \frac{1}{2}\gamma_{il}\gamma_{kj}, \tag{62}$$

which is a two-body cumulant. Moreover, the extended normal ordering is not well defined for multiple states. Despite all these downsides, it is straightforwardly extensible to non-linear wavefunctions such as MRCC, unlike Equation (58). In this review, we will not further investigate this case.

In summary, using Equations (49) and (59) the geminal part of the wavefunction, as used in the present work, takes the form

$$\hat{Q}\hat{F}|0\rangle = \sum_{ijp}\sum_{\alpha\beta} \mathcal{T}_{\alpha\beta}^{ijp}\hat{E}_{ijp}^{\alpha\beta}|0\rangle + \sum_{S,x}\mathcal{F}_x^S|S^x\rangle. \tag{63}$$

7. Working equations

Given the parametrisation of the wavefunction, we now present the working equations for the various MR-F12 methods [33–35] and discuss the approximations that are necessary for an efficient implementation.

7.1. The CASPT2-F12 method

The CASPT2-F12 method [33] can be seen as a minimisation of the Hylleraas functional, cf. Equation (16) with respect to the parameters of the first-order wavefunction ($|\Psi^{(1)}\rangle = |\Psi\rangle - |0\rangle$) subject to the intermediate normalisation, $\langle 0|\Psi\rangle = 1$, which implies $t_{\mathrm{F12}} = 1$ (cf. Equation 56). The projected Fock operator,

$$\hat{H}^{(0)} = \hat{P}\hat{f}\hat{P} + (1-\hat{P})\hat{f}(1-\hat{P}), \tag{64}$$

$$\begin{aligned}\hat{f} &= \sum_{\kappa\lambda} f_{\kappa\lambda}\hat{E}_{\kappa\lambda} \\ &= \sum_{\kappa\lambda}\left[h_{\kappa\lambda} + \sum_{ij}\gamma_{ij}^{\mathrm{sa}}\left(J_{\kappa\lambda}^{ij} - \tfrac{1}{2}K_{\kappa\lambda}^{ij}\right)\right]\hat{E}_{\kappa\lambda},\end{aligned} \tag{65}$$

with $\hat{P} = |0\rangle\langle 0|$ is used in this review for the zeroth-order Hamiltonian. This choice, which is formally arbitrary, defines the perturbation theory. Other choices are possible as well (e.g. the Dyall Hamiltonian [124] as used in NEV-PT [19–21]), and of course the definition of $H^{(0)}$ affects the results.

The projection operators ensure that the reference function is an eigenfunction of $\hat{H}^{(0)}$, i.e.

$$\hat{H}^{(0)}|0\rangle = E^{(0)}|0\rangle. \tag{66}$$

The amplitude equations for the amplitudes of the conventional configurations are obtained by taking the derivatives with respect to the parameters t_I, t_a^S and t_{ab}^{ij}. In analogy to Equations (18)–(20), they can be written as

$$R_{ab}^{Dp} = \langle \Phi_{Dp}^{ab}|\hat{H}|0\rangle + \langle \Phi_{Dp}^{ab}|\hat{H}^{(0)} - E^{(0)}|\Psi_{\text{conv}}\rangle + C_{ab}^{Dp} = 0, \tag{67}$$

$$r_a^S = \langle S^a|\hat{H}|0\rangle + \langle S^a|\hat{H}^{(0)} - E^{(0)}|\Psi_{\text{conv}}\rangle + C_a^S = 0, \tag{68}$$

$$r_I = \langle I|\hat{H}|0\rangle + \langle I|\hat{H}^{(0)} - E^{(0)}|\Psi_{\text{conv}}\rangle + C_I = 0, \tag{69}$$

where the indices Dp refer to orthogonalised configurations as defined in Equation (23), and in the last equation I excludes the reference CSFs. This means that the projection to the internal CSFs (Equation 69) is entirely omitted when a CASSCF reference function is used and there are no closed-shell (inactive) correlated orbitals. The equations are solved iteratively as outlined in Section 2.

The difference between the conventional and explicitly correlated CASPT2 equations is the C tensors arising from the coupling between the conventional and geminal excitations through the zeroth-order Hamiltonian. Their explicit expressions are as follows:

$$C_{ab}^{Dp} = \langle \Phi_{Dp}^{ab}|\hat{H}^{(0)}\hat{Q}\hat{F}|0\rangle = \sum_x \left(f_{ax}\mathcal{F}_{xb}^{Dp} + \mathcal{F}_{ax}^{Dp} f_{xb} \right), \tag{70}$$

$$C_a^S = \langle S^a|\hat{H}^{(0)}\hat{Q}\hat{F}|0\rangle = \sum_x f_{ax}\mathcal{F}_x^S + 2\sum_x \sum_{ijp,k} \mathcal{F}_{ax}^{ijp} f_{xk}\sigma_k(ijp, S) \tag{71}$$

$$C_I = \langle I|\hat{H}^{(0)}\hat{Q}\hat{F}|0\rangle = \sum_{x,k}\sum_S f_{kx}\mathcal{F}_x^S\sigma_k(S, I). \tag{72}$$

The integrals arising in these and the following equations are defined in Table 2, and the coupling coefficients such as σ_k are summarised in Table 3. Due to the different definitions of the semi-internal geminal excitations, the explicit expressions for the matrix elements given here are different from those in the original publication [33].

Table 2. Definition of the integrals used in the F12 formalism.

$J_{\kappa\lambda}^{kl} = \langle \kappa k|r_{12}^{-1}|\lambda l\rangle$
$K_{\kappa\lambda}^{kl} = \langle \kappa\lambda|r_{12}^{-1}|kl\rangle$
$F_{\kappa\lambda}^{kl} = \langle \kappa\lambda|F_{12}|kl\rangle$
$W_{\kappa\lambda}^{kl} = \langle \kappa\lambda|r_{12}^{-1}F_{12}|kl\rangle$
$F_{ij,kl}^2 = \langle ij|F_{12}^2|kl\rangle$
$V_{\kappa\lambda}^{ij} = \langle \kappa\lambda|r_{12}^{-1}\hat{Q}_{12}F_{12}|ij\rangle = W_{\kappa\lambda}^{ij} - K_{\kappa\lambda}^{rs}F_{rs}^{ij} - K_{\kappa\lambda}^{ox}F_{ox}^{ij} - K_{\kappa\lambda}^{xo}F_{xo}^{ij}$
$X_{ij,kl} = \langle ij|F_{12}\hat{Q}_{12}F_{12}|kl\rangle = F_{ij,kl}^2 - F_{rs}^{ij}F_{rs}^{kl} - F_{ox}^{ij}F_{ox}^{kl} - F_{xo}^{ij}F_{xo}^{kl}$
$B_{ij,kl} = \langle ij|F_{12}\hat{Q}_{12}(\hat{f}_1 + \hat{f}_2)\hat{Q}_{12}F_{12}|kl\rangle$
$\mathcal{F}_{\kappa\lambda}^{ijp} = \frac{1}{2}t_{ijp}\left(F_{\kappa\lambda}^{ij} + pF_{\kappa\lambda}^{ji}\right)$
$\mathcal{V}_{\kappa\lambda}^{ijp} = \frac{1}{2}t_{ijp}\left(V_{\kappa\lambda}^{ij} + pV_{\kappa\lambda}^{ji}\right)$
$\mathcal{X}_{ijp,klq} = \frac{1}{2}\delta_{pq}t_{ijp}t_{klq}\left(X_{ij,kl} + pX_{ji,kl}\right)$
$\mathcal{B}_{ijp,klq} = \frac{1}{2}\delta_{pq}t_{ijp}t_{klq}\left(B_{ij,kl} + pB_{ji,kl}\right)$

Table 3. Definition of the coupling coefficients used in this review. All quantities are independent of the external indices a, b. The coupling coefficients are the same as used in the conventional MR methods.

Pair–pair:	$\gamma(ijp, klq) = \delta_{pq}f_{mn}\langle 0|\hat{E}_{kln}^{ijm} + p\hat{E}_{kln}^{jim}|0\rangle$
Single–single:	$\gamma(S, T) = f_{mn}\langle S^a|\hat{E}_n^m|T^a\rangle$
Pair–single:	$\sigma_k(ijp, S) = \langle \Phi_{ijp}^{ab}|\hat{E}_k^b|S^a\rangle$
Pair–internal:	$\sigma_{mn}(ijp, I) = \frac{1}{2}\langle 0|\hat{E}_{mn}^{ij} + p\hat{E}_{nm}^{ij}|I\rangle$
Single–internal:	$\sigma_k(S, I) = \langle S^a|\hat{E}_k^a|I\rangle$
	$\alpha_{kmn}(S, I) = \langle S^a|\hat{E}_{kn}^{am}|I\rangle$
Pair–ref.:	$\sigma_{mn}(ijp, 0) = \frac{1}{2}\langle 0|\hat{E}_{mn}^{ij} + p\hat{E}_{nm}^{ij}|0\rangle$

The CASPT2 energy expression is also augmented by the F12 contributions

$$E_{\text{CASPT2–F12}} = E_{\text{CASPT2}} + E_{\text{F12}} \tag{73}$$

where the F12 contributions E_{F12} can be decomposed as

$$E_{\text{F12}} = 2\langle \Psi_{\text{conv}}|\hat{H}^{(0)}\hat{Q}\hat{F}|0\rangle + \langle 0|\hat{F}^\dagger\hat{Q}\hat{H}^{(0)}\hat{Q}\hat{F}|0\rangle - E_0\langle 0|\hat{F}^\dagger\hat{Q}\hat{F}|0\rangle + 2\langle 0|\hat{F}^\dagger\hat{Q}\hat{H}|0\rangle. \tag{74}$$

Note that E_{CASPT2} differs from the conventional CASPT2 energy, since the amplitudes are different due to the coupling terms in the amplitude equations. This is very similar to the single-reference MP2-F12 theory. The explicit formulae are the following:

$$\langle \Psi_{\text{conv}}|\hat{H}^{(0)}\hat{Q}\hat{F}|0\rangle = \sum_{Dp,ab} t_{ab}^{Dp}C_{ab}^{Dp} + \sum_{S,a} t_a^S C_a^S + \sum_I t_I C_I, \tag{75}$$

$$\langle 0|\hat{F}^\dagger \hat{Q} \hat{H}^{(0)} \hat{Q} \hat{F}|0\rangle$$
$$= \sum_{ijp,klp} \left[\mathcal{B}_{ijp,klq} S_{ijp,klq} + \mathcal{X}_{ijp,klq} \gamma(ijp, klq)\right]$$
$$+ 4 \sum_{ijp,k} \sum_{ax} \sum_{S} \mathcal{F}_x^S \left[f_{ak} \mathcal{F}_{xa}^{ijp} + f_{yk} \mathcal{F}_{xy}^{ijp}\right] \sigma_k(ijp, S)$$
$$+ \sum_{xy} \sum_{S} \mathcal{F}_x^S f_{xy} \mathcal{F}_y^S + \sum_{x} \sum_{ST} \mathcal{F}_x^S \mathcal{F}_x^T \gamma(S, T), \quad (76)$$

$$\langle 0|\hat{F}^\dagger \hat{Q} \hat{F}|0\rangle = \sum_{ijp,klq} \mathcal{X}_{ijp,klq} S_{ijp,klq}, \quad (77)$$

$$\langle 0|\hat{F}^\dagger \hat{Q} \hat{H}|0\rangle = \sum_{ijp,kl} \mathcal{V}_{kl}^{ijp} \sigma_{kl}(ijp, 0) + \sum_{x} \sum_{S} \mathcal{F}_x^S p_x^S, \quad (78)$$

where we have introduced $p_x^S = \langle S^x|\hat{H}|0\rangle$.

In summary, the following should be pointed out: (i) All expressions given above involve only the same coupling coefficients and density matrices as needed in conventional CASPT2, and therefore the evaluation of the C tensors and of the F12 energy contributions takes little extra effort, once all required F12 integrals and intermediates are available. (ii) The matrices V_{kl}^{ij}, $B_{ij,kl}$ and $X_{ij,kl}$ are exactly the same as in the closed-shell single-reference MP2-F12 theory, except that they are needed here for all k, l, while in MP2-F12 only $kl = ij$ and $kl = ji$ are required (in the diagonal or FIX approximations [81]). However, exactly the same basic integrals such as $F_{\kappa\lambda}^{kl}$, $W_{\kappa\lambda}^{kl}$, $F_{ij,kl}^2$ have to be computed in both cases, and this dominates the computational effort. $B_{ij,kl}$ is evaluated using the so-called approximation C [85, 81]. The working equations can be found in Ref. [81].

In total, the extra computational effort for the F12 treatment in CASPT2 is comparable to MP2-F12. In MP2-F12, the F12 part is typically one order of magnitude more expensive than standard MP2, while in CASPT2-F12 the relative effort decreases with increasing active space and the number of reference CSFs. The CPU-time for MP2-F12 or CASPT2-F12 is usually still less than that for a conventional calculation with a basis set that yields comparable accuracy. It should be noted, however, that often in MP2 or CASPT2 the basis-set incompleteness errors do not dominate the total errors, and therefore the F12 treatment does not necessarily improve the overall accuracy. This is entirely different in higher level methods such as CCSD(T)-F12 or MRCI-F12 which have much smaller intrinsic errors, and therefore their overall accuracy is strongly dependent on the quality of the basis set.

7.2. The MRCI-F12 method

In the MRCI-F12 method [34, 35] the energy expectation value

$$E_{\mathrm{MRCI}} = \frac{\langle\Psi|\hat{H}|\Psi\rangle}{\langle\Psi|\Psi\rangle} = \frac{\langle\Psi_{\mathrm{conv}}|\hat{H}|\Psi_{\mathrm{conv}}\rangle + 2At_{\mathrm{F12}} + Bt_{\mathrm{F12}}^2}{\langle\Psi_{\mathrm{conv}}|\Psi_{\mathrm{conv}}\rangle + Xt_{\mathrm{F12}}^2} \quad (79)$$

is minimised with respect to all wavefunction parameters. Here we have introduced the following quantities:

$$A = \langle\Psi_{\mathrm{conv}}|\hat{H}\hat{Q}\hat{F}|0\rangle, \quad (80)$$

$$B = \langle 0|\hat{F}^\dagger \hat{Q}\hat{H}\hat{Q}\hat{F}|0\rangle, \quad (81)$$

$$X = \langle 0|\hat{F}^\dagger \hat{Q}\hat{F}|0\rangle. \quad (82)$$

Also the parameter t_{F12} is optimised variationally. Since effectively the fixed amplitudes in Equation (44) are scaled by t_{F12}, we denote this as the *scaled fixed amplitude ansatz* (SFIX). It yields the best possible variational energy for the chosen wavefunction ansatz, despite the fact that the first-order cusp conditions may not be exactly fulfilled. Furthermore, this method can be straightforwardly extended to MS treatments, as described in Section 7.3. It should be noted, however, that the F12 energy correction is not size-consistent, but since the variational MRCI energy is not size-consistent anyway, this does not introduce a serious additional problem.

Alternatively, one can ensure that the first-order cusp conditions are exactly fulfilled. In this case, the factor t_{F12} is fixed to unity, and the intermediate normalisation condition is imposed by minimising the Lagrangian functional

$$L = E_{\mathrm{MRCI}} + \lambda(\langle\Psi|0\rangle - 1). \quad (83)$$

This yields an F12 energy contribution that satisfies exactly the first-order cusp conditions, and it is denoted as the *fixed amplitude ansatz* (FIX).

The residual equations for the conventional amplitudes are in case of the SFIX ansatz

$$R_{ab}^{Dp} = \langle\Phi_{Dp}^{ab}|\hat{H}|\Psi_{\mathrm{conv}}\rangle + A_{ab}^{Dp} t_{\mathrm{F12}} - E t_{ab}^{Dp} = 0, \quad (84)$$

$$r_a^S = \langle S^a|\hat{H}|\Psi_{\mathrm{conv}}\rangle + A_a^S t_{\mathrm{F12}} - E t_a^S = 0, \quad (85)$$

$$r_I = \langle I|\hat{H}|\Psi_{\mathrm{conv}}\rangle + A_I t_{\mathrm{F12}} - E t_I = 0. \quad (86)$$

The coefficient t_{F12} is given directly by

$$t_{\mathrm{F12}} = \frac{-A}{(B - EX)}. \quad (87)$$

In the FIX case, one has by definition $t_{\mathrm{F12}} = 1$, and the residuals r^R for the reference configurations ($R \in I$) are augmented by a term $-\lambda t_R^{(0)}$, where $t_R^{(0)}$ are the coefficients of the reference configurations in the fixed reference function. The A tensors are defined formally as

$$A_{ab}^{Dp} = \langle\Phi_{Dp}^{ab}|\hat{H}\hat{Q}\hat{F}|0\rangle, \quad (88)$$

$$A_a^S = \langle S^a|\hat{H}\hat{Q}\hat{F}|0\rangle, \quad (89)$$

$$A_I = \langle I|\hat{H}\hat{Q}\hat{F}|0\rangle, \quad (90)$$

and from these the scalar quantity A (cf. Equation 80) is obtained by taking the scalar product with the amplitudes:

$$A = \sum_I t_I A_I + \sum_a \sum_S t_a^S A_a^S + \sum_{ab} \sum_{Dp} t_{ab}^{Dp} A_{ab}^{Dp}. \quad (91)$$

In order to arrive at computationally efficient equations, it is necessary to introduce approximations for the quantities A_a^S, A_{ab}^{Dp} and B. These are very similar to those in approximate CCSD-F12 theories. We have used the so-called approximation F12x [86, 125] to evaluate the A_{ab}^{Dp} and A_a^S tensors. This yields

$$A_{ab}^{Dp} \approx \bar{\mathcal{V}}_{ab}^{Dp} + C_{ab}^{Dp}, \quad (92)$$

$$A_a^S \approx 2 \sum_{ijp,k} \bar{\mathcal{V}}_{ak}^{ijp} \sigma_k(ijp, S) + C_a^S, \quad (93)$$

where C_{ab}^{Dp} and C_a^S have been defined in Equations (70) and (71). The $\mathcal{V}^{ijp}$ intermediates are approximated by

$$\bar{\mathcal{V}}_{rs}^{ijp} = \frac{1}{2} t_{ijp} \left(\bar{V}_{rs}^{ij} + p \bar{V}_{rs}^{ji} \right), \quad (94)$$

$$\bar{V}_{rs}^{ij} = W_{rs}^{ij} - \sum_{tu} K_{rs}^{tu} F_{tu}^{ij}. \quad (95)$$

The approximation in Equation (95) is that contributions of integrals $\langle xo|r_{12}^{-1}|rs\rangle$ and $\langle ox|r_{12}^{-1}|rs\rangle$, which contain up to two virtual orbitals and one CA orbital, are neglected. These terms arise from the last two terms in the projector in Equation (42). It has been found for CCSD-F12 that these contributions are very small and normally negligible as compared to other errors [125]. The advantage is that the remaining terms, which involve integrals with up to four external orbitals, can be evaluated together with similar contractions $\sum_{ab} K_{tu}^{ab} T_{ab}^{ij}$, which arise in standard MRCI, with negligible additional computational effort. In order to avoid the transformation of the four-index integrals into the molecular orbital (MO) basis, these terms are evaluated directly from the integrals in the atomic orbital (AO) basis as

$$\sum_{ab} K_{rs}^{ab} T_{ab}^{ij} - \sum_{tu} K_{rs}^{tu} F_{tu}^{ij} = \sum_{\mu\nu} C_{\mu r} C_{\nu s} \sum_{\rho\sigma} \langle \mu\nu | r_{12}^{-1} | \rho\sigma \rangle \left[T_{\rho\sigma}^{ij} - F_{\rho\sigma}^{ij} \right], \quad (96)$$

$$T_{\rho\sigma}^{ij} = \sum_{ab} C_{\rho a} T_{ab}^{ij} C_{\sigma b}, \quad (97)$$

$$F_{\rho\sigma}^{ij} = \sum_{tu} C_{\rho t} F_{tu}^{ij} C_{\sigma u}. \quad (98)$$

The quantities A_I are evaluated without approximations, since $\langle 0|\hat{H}\hat{Q}\hat{F}|0\rangle = \sum_R c^R A^R$ contributes directly to the energy. The explicit expression involves integrals $J_{kx}^{mn} = \langle mk|r_{12}^{-1}|nx\rangle$ and reads

$$A_I = \sum_x \sum_S \left[\sum_k h_{kx} \sigma_k(S, I) + \sum_{kmn} J_{kx}^{mn} \alpha_{kmn}(S, I) \right] \mathcal{F}_x^S + \sum_{ijp,mn} \mathcal{V}_{mn}^{ijp} \sigma_{mn}(ijp, I). \quad (99)$$

We also approximate the energy expression in a manner that is consistent with F12b. The scalar B is computed by replacing the normal-ordered Hamiltonian with the normal-ordered Fock operator, i.e.

$$B \approx (E_{\rm ref} - E^{(0)}) X + \langle 0|\hat{F}^\dagger \hat{Q} \hat{f} \hat{Q} \hat{F}|0\rangle, \quad (100)$$

where $E^{(0)}$ is the zeroth-order energy as in CASPT2. The last term is evaluated as shown in Equation (76), and X as in Equation (77).

7.3. *Multistate extension of the MRCI-F12 method*

In the presence of strong state mixings, e.g. around conical intersections and avoided crossings, the reference functions are strongly mixed in the correlated wavefunctions. Therefore, it is important to parametrise the wavefunction in an invariant way with respect to rotations among the reference functions. As already outlined in Section 3, this can be achieved by generating the internally contracted configurations from all the reference functions $|0_M\rangle$, and using the union of these to expand the wavefunction [54]:

$$|\Psi_N\rangle = \sum_I t_I^N |I\rangle + \sum_{S,a} t_a^{S,N} |S^a\rangle + \sum_M^{\rm ref} \sum_{ijp,ab} t_{ab}^{ijp,NM} |\Phi_{ijp,M}^{ab}\rangle + \sum_M^{\rm ref} t_{\rm F12}^{NM} \hat{Q}\hat{F}|0_M\rangle, \quad (101)$$

where the internally contracted basis is

$$|\Phi_{ijp,M}^{ab}\rangle = \hat{E}_{ijp}^{ab} |0_M\rangle. \quad (102)$$

All the formulae stay the same except that one needs to evaluate transition density matrices of the type

$$\gamma_{ij}^{MN} = \langle 0_M | \hat{E}_j^i | 0_N \rangle, \quad (103)$$

$$\Gamma_{ij,kl}^{MN} = \langle 0_M | \hat{E}_{jl}^{ik} | 0_N \rangle, \quad (104)$$

and so on. The metric in the projector in Equation (58) is replaced by all the blocks of the transition density matrices as well.

Special care must be taken for the geminal–geminal block of the Hamiltonian matrix. We compute it by means of the following formula:

$$B_{MN} \approx \frac{1}{2}\left(E_M^{\mathrm{ref}} + E_N^{\mathrm{ref}} - E_M^{(0)} - E_N^{(0)}\right)\langle 0_M|\hat{F}^\dagger\hat{Q}\hat{F}|0_N\rangle + \langle 0_M|\hat{F}^\dagger\hat{Q}\hat{f}\hat{Q}\hat{F}|0_N\rangle, \quad (105)$$

which is analogous to the MS-CASPT2 formula [5, 15]. Unfortunately, this approximation breaks the invariance of the internally contracted MRCI theory with respect to the rotation of reference functions, which implies that we need to choose a most suitable set of reference functions. In a recent study [35, 55], we have realised that the naive choice of the CASSCF reference functions may lead to humps on the PESs around the points where the CASSCF surfaces cross each other. This is due to the fact that although the potentials E_N^{ref} are smooth, $E_N^{(0)}$ (the expectation values of the Fock operator) change dramatically around the CASSCF crossing points. We have therefore chosen to use a set of reference functions that diagonalise the zeroth-order Hamiltonian within the reference space:

$$|0_M\rangle = \sum_N |0_N^{\mathrm{CASSCF}}\rangle U_{NM}, \quad (106)$$

$$[\mathbf{U}^\dagger\mathbf{H}^{(0)}\mathbf{U}]_{MN} = \delta_{MN}E_M^{(0)}. \quad (107)$$

This procedure is related to the recently proposed 'extended' MCQDPT2 method of Granovsky [38] and its XMS-CASPT2 counterpart developed by us [36, 37]. For further details, see Refs. [35, 55].

8. Size-consistency corrections

8.1. Davidson corrections

A severe problem of the MRCI-F12 method is its lack of size consistency. Various schemes have been proposed in the literature that reduce the size-consistency errors, without substantially increasing the computational effort. The simplest possibility is to apply a posteriori the multireference Davidson correction [126], which accounts for contributions of higher order excitations. This has been implemented for MRCI-F12 in the same way as in the conventional MRCI method [127]. The correction is defined as

$$\Delta E_N^{+\mathrm{Q}} = (E_N - E_N^{\mathrm{ref}})/(c_N)^2, \quad (108)$$

where c_N is the coefficient of the reference function in the (normalised) MRCI-F12 wavefunction for state N. One can either use the fixed reference function, yielding

$$c_N = \frac{1}{\sqrt{N}}\langle 0_N|\Psi_N\rangle = \frac{1}{\sqrt{N}}\sum_{I\in\{R\}} t_I^{(0)}t_I, \quad (109)$$

in which $N = \langle\Psi_N|\Psi_N\rangle$ (Q1 correction in Ref. [127]). This may fail in the vicinity of conical intersections, since then states may strongly mix and c_N may get small, leading to a strong overestimation of the correction. This problem can be avoided by using instead of the coefficients $t_I^{(0)}$ the relaxed reference coefficients t_I. Renormalisation of the relaxed reference function then yields

$$(c_N)^2 = \frac{1}{N}\sum_{I\in\{R\}}(t_I^N)^2 \quad (110)$$

(Q0 correction in Ref. [127]). This correction is used by default, unless otherwise stated.

Furthermore, in cases of strong state mixings the reference energy E_N^{ref} should be replaced by $\tilde{E}_{\mathrm{ref}}^M = \langle\tilde{M}|\hat{H}|\tilde{M}\rangle$, where the rotated reference states $|\tilde{M}\rangle$ are obtained by a unitary transformation of the original reference functions that maximises the overlap with the final MRCI-F12 wavefunctions:

$$|\tilde{M}\rangle = \sum_N |0_N\rangle\left[\mathbf{T}(\mathbf{T}^\dagger\mathbf{T})^{-1/2}\right]_{NM}, \quad (111)$$

$$T_{NM} = \langle 0_N|\Psi_M\rangle. \quad (112)$$

This takes care of the fact that the order of the states may be different for the MRCI-F12 and CASSCF reference wavefunctions. Nevertheless, it can still happen that the Davidson-corrected energies show an unphysical behaviour near narrow avoided crossings or conical intersections; they may even cross for states of the same symmetry. See Ref. [127] for more details.

8.2. MRACPF-F12 and related schemes

While the Davidson correction is computed using the converged MRCI-F12 wavefunction, other schemes have been proposed in which a modified, approximately size-consistent, energy functional is minimised. In the MRACPF-F12 method, proposed by Gdanitz and Ahlrichs [128], one uses

$$E = E_{\mathrm{ref}} + \frac{\langle\Psi|H - E_{\mathrm{ref}}|\Psi\rangle}{\langle 0|0\rangle + g_a\langle\Psi_{\mathrm{int}}|\Psi_{\mathrm{int}}\rangle + g_e\langle\Psi_{\mathrm{ext}}|\Psi_{\mathrm{ext}}\rangle} + \lambda(\langle\Psi|0\rangle - 1), \quad (113)$$

where

$$|\Psi_{\mathrm{int}}\rangle = (1 - \hat{P}_0)\sum_I t_I|I\rangle, \quad (114)$$

$$|\Psi_{\mathrm{ext}}\rangle = \sum_{S,a} t_a^S|S^a\rangle + \sum_{ijp,ab} t_{ab}^{ijp}|\Phi_{ijp}^{ab}\rangle + t_{\mathrm{F12}}\hat{Q}\hat{F}|0\rangle. \quad (115)$$

We use the FIX ansatz, i.e. $t_{\mathrm{F12}} = 1$ with intermediate normalisation. Taking the derivatives with respect to the t amplitudes leads to the amplitude equations, which differ from those for the corresponding MRCI-F12 only in the terms that contain the energy:

$$\langle \Phi_{Dp}^{ab} | \hat{H} | \Psi_{\mathrm{conv}} \rangle + A_{ab}^{Dp} t_{\mathrm{F12}} - \epsilon_e t_{ab}^{Dp} = 0, \quad (116)$$

$$\langle S^a | \hat{H} | \Psi_{\mathrm{conv}} \rangle + A_a^S t_{\mathrm{F12}} - \epsilon_e t_a^S = 0, \quad (117)$$

$$\langle I | \hat{H} | \Psi_{\mathrm{conv}} \rangle + A_I t_{\mathrm{F12}} - \lambda t_I^{(0)} - \epsilon_a t_I = 0, \quad (118)$$

where ϵ_e and ϵ_a are defined as

$$\epsilon_a = E_{\mathrm{ref}} + g_a(E - E_{\mathrm{ref}}), \quad (119)$$

$$\epsilon_e = E_{\mathrm{ref}} + g_e(E - E_{\mathrm{ref}}). \quad (120)$$

In the MRACPF model, the factors g_e and g_a are (n is the number of electrons)

$$g_a = 1, \quad (121)$$

$$g_e = \frac{2}{n}, \quad (122)$$

while the MRAQCC model [129] uses the factors

$$g_a = 1, \quad (123)$$

$$g_e = 1 - \frac{(n-2)(n-3)}{n(n-1)}. \quad (124)$$

All the matrix elements are evaluated in exactly the same way as in MRCI-F12. So far, we have only implemented these methods for SS calculations.

9. CABS singles corrections

In most cases, the difference between the MRCI-F12 energy obtained with medium-size basis sets and the corresponding CBS limit is dominated by the basis-set truncation error in the CASSCF reference energy rather than in the MRCI-F12 correlation energy. It is therefore important to apply a basis-set correction also to the reference energies. This is analogous to single-reference CC-F12 methods in which a perturbative correction can be added to the HF energy (the so-called CABS singles correction [86, 87]).

In the multireference case, the calculation of such basis-set corrections is less straightforward than in the single-reference case since the first derivatives of the energy with respect to unitary orbital transformations cannot be expressed by a single Fock operator. The first such correction on top of CASSCF has been proposed by Kong and Valeev, who have used a perturbative approach [89]. We have investigated various other possibilities, two of which are presented here for the first time.

Our preferred correction is computed for each state separately through a singles CI, as was first described in Ref. [33]. The singles CI wavefunction is expanded by the reference and internally contracted singles functions

$$|\tilde{\Phi}_{i,N}^x\rangle = \hat{E}_i^x |\tilde{N}\rangle\,. \quad (125)$$

In multistate calculations, we generate the singles from all the references, so that this basis is invariant with respect to unitary transformations among the reference functions. These internally contracted CABS singles configurations are orthogonal to the space considered in MRCI-F12, since they are projected out from the singles geminal functions [cf. Equation (58)].

The CABS singles wavefunction for state M is defined as

$$|\Psi_S^M\rangle = |\tilde{M}\rangle + \sum_{i,x} \sum_N t_x^{i,MN} |\tilde{\Phi}_{i,N}^x\rangle. \quad (126)$$

Note that the first term is state-specific and uses the rotated reference wavefunction $|\tilde{M}\rangle$ that has largest overlap with the MRCI-F12 wavefunction for state M (cf. Equation 111). Note that these rotated reference functions are also used in the definition of the singles configurations, which is convenient in the following expressions.

The amplitudes in Equation (126) are optimised by minimising the energy expectation value $E_S^M = \langle \Psi_S^M | \hat{H} | \Psi_S^M \rangle / \langle \Psi_S^M | \Psi_S^M \rangle$, i.e. by solving the eigenvalue equation

$$\langle \tilde{\Phi}_{i,N}^x | \hat{H} - E_S^M | \Psi_S^M \rangle = 0, \quad (127)$$

The necessary matrix elements are

$$\langle \tilde{M} | \hat{H} | \tilde{\Phi}_{i,N}^x \rangle = \sum_j \tilde{\gamma}_{ji}^{MN} h_{xj} + \sum_{jkl} \tilde{\Gamma}_{ji,kl}^{MN} J_{xj}^{kl}, \quad (128)$$

$$\langle \tilde{\Phi}_{i,N}^x | \hat{H} | \tilde{\Phi}_{j,L}^y \rangle = h_{xy} \tilde{\gamma}_{ij}^{NL} + \sum_{kl} \left(\tilde{\Gamma}_{ij,kl}^{NL} J_{xy}^{kl} + \tilde{\Gamma}_{kj,il}^{NL} K_{xy}^{kl} \right) + \delta_{xy} \sum_{kl} \tilde{\Gamma}_{ij,kl}^{NL} h_{kl} + \frac{1}{2} \delta_{xy} \sum_{klmn} \tilde{\Gamma}_{ij,kl,mn}^{NL} J_{mn}^{kl}. \quad (129)$$

The transition density matrices $\tilde{\gamma}_{ij}^{MN}$, $\tilde{\Gamma}_{ij,kl}^{MN}$ and $\tilde{\Gamma}_{ijk,lmn}^{MN}$ are computed using the rotated reference functions

$$\tilde{\gamma}_{ij}^{MN} = \langle \tilde{M} | \hat{E}_j^i | \tilde{N} \rangle, \quad (130)$$

$$\tilde{\Gamma}_{ij,kl}^{MN} = \langle \tilde{M} | \hat{E}_{jl}^{ik} | \tilde{N} \rangle, \quad (131)$$

$$\tilde{\Gamma}_{ij,kl,mn}^{MN} = \langle \tilde{M} | \hat{E}_{jln}^{ikm} | \tilde{N} \rangle. \quad (132)$$

The singles correction is then defined as

$$\Delta E_S^M = E_S^M - \langle \tilde{M}|\hat{H}|\tilde{M}\rangle. \quad (133)$$

Alternatively, one can perform perturbative corrections similar to those by Kong and Valeev [89], generalised here for MS cases, using the zeroth-order Hamiltonian

$$\hat{H}^{(0)} = \sum_{rs} f_{rs}\hat{E}_{rs} + \sum_{xy} f_{xy}\hat{E}_{xy}. \quad (134)$$

The working equation of this approach is

$$\langle \tilde{\Phi}_{i,N}^x|\hat{H}^{(0)} - \tilde{E}_M^{(0)}|\Psi_S^M\rangle + \langle \tilde{\Phi}_{i,N}^x|\hat{H}|\tilde{M}\rangle = 0, \quad (135)$$

$$\Delta E_S^M \equiv E_M^{(2)} = \langle \tilde{M}|\hat{H}|\Psi_S^M\rangle. \quad (136)$$

One can also include $\sum_{xa} f_{xa}(\hat{E}_{xa} + \hat{E}_{ax})$ in the zeroth-order Hamiltonian as in the formula of Kong and Valeev, or, in turn, as in the original CABS singles formula in the single reference framework [86, 125], but we observe only a marginal difference in the performance for relative energies. The matrix elements are obtained from those for the singles CI by replacing $h_{\kappa\lambda}$ by $f_{\kappa\lambda}$ and omitting all contributions of two-electron integrals.

The perturbative approach has the advantage that the computation of the J^{kl} and K^{kl} integrals with two CABS indices can be avoided. However, the introduction of the Fock operator in the singles correction may amplify the breaking of degeneracies of states with different spatial symmetries, because the Fock operator is not totally symmetric within the degeneracy manifold, unless the density matrix used to construct the Fock operator is totally symmetric. Note that often the states within one irreducible representation do not give totally symmetric density matrices.

Finally, we have implemented a variant of MRCI-F12 that includes the singles $|\Phi_{i,N}^x\rangle$ directly in the wave-function ansatz and in which the singles amplitudes are determined in the iterative MRCI-F12 diagonalisation ('iterative' scheme). In order to avoid an unnecessary computational demand, we neglect interactions between the external configurations and the CABS singles configurations.

As an example, these three corrections have been used to compute the LiF avoided crossing at a long distance (cf. Figure 1). Using a double-ζ basis set (cc-pVDZ for Li and aug-cc-pVDZ for F) with the corresponding CABS basis sets [130], all CABS singles corrections give rise to problems: (i) both the CI and PT corrections have wiggles due to the uncoupled nature of these corrections; (ii) the curves from the iterative correction are smooth, but seem to suffer severely from the size-consistency error, resulting in a crossing at a much shorter bond length. Note that the absolute size of the singles correction with this small basis is about 30 mH, which is very large on the scale of the figure. With the corresponding triple-ζ basis sets, the singles corrections are so small that all three corrections essentially give the same curves.

It should be noted that in the MS case the CABS singles correction does not represent a correction for the basis-set incompleteness errors of the CASSCF energies obtained with state-averaged orbitals. This is because our current methods are state-specific, and the singles correction may also account for part of the error caused by the state-averaging. It should be possible to devise alternative correction schemes in which a CABS correction is computed for the state-averaged orbitals, and the corrected orbitals are then used to compute the individual energies. One could also include the relaxation of the CASSCF configuration coefficients. This would basically correspond to performing one CASSCF iteration in the OBS+CABS basis. We plan to investigate such schemes in future work.

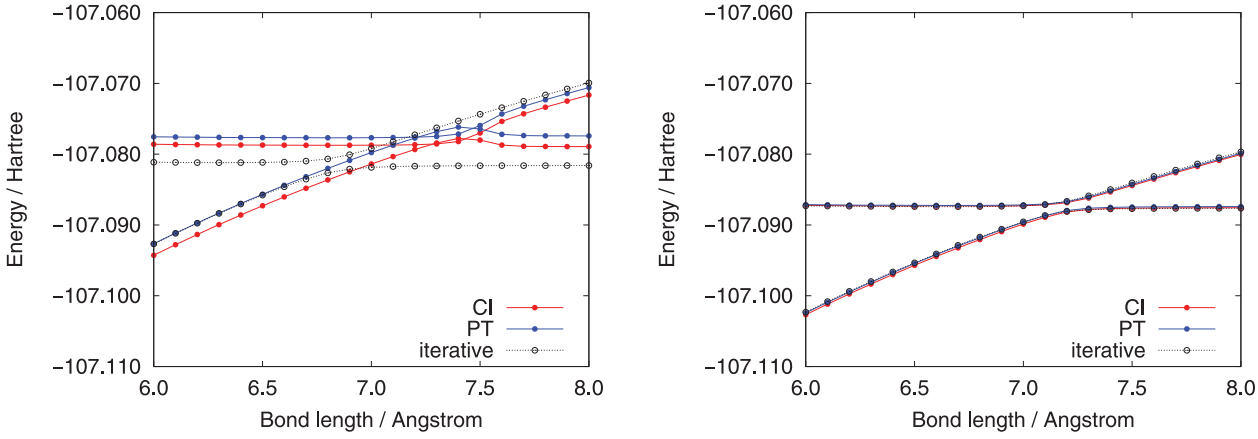

Figure 1. Comparison of three CABS singles corrections using double-ζ (left-hand panel) and triple-ζ (right-hand panel) basis sets. CI (red lines) denotes the singles-CI correction, PT (blue lines), the perturbative correction, and 'iterative' (black lines), the iterative correction (see text).

Table 4. Vertical excitation energies (in eV) for low-lying A_1 and B_2 states of pyrrole with six electrons in four b_1 and three a_2 active orbitals. The CASPT2 and CASPT2-F12 results were taken from Ref. [33].

OBS	A_1 $1a_2 \rightarrow 3p_x$	A_1 $2b_1 \rightarrow 3p_x$	B_2 $1a_2 \rightarrow 3p_x$	B_2 $2b_1 \rightarrow 3p_x$	B_2 $\pi \rightarrow \pi^*$
			CASSCF		
VDZ-F12+	5.57	5.68	4.87	6.34	8.00
VTZ-F12+	5.59	5.70	4.88	6.37	8.00
VQZ-F12+	5.58	5.70	4.88	6.36	7.99
			CASPT2		
VDZ-F12+	6.69	6.81	6.00	7.61	6.03
VTZ-F12+	6.86	6.98	6.16	7.79	5.98
VQZ-F12+	6.92	7.04	6.21	7.85	5.97
			CASPT2-F12		
VDZ-F12+	6.96	7.09	6.26	7.90	5.99
VTZ-F12+	6.98	7.11	6.27	7.92	5.98
VQZ-F12+	6.98	7.10	6.27	7.92	5.97
			MRCI+Q[a]		
VDZ-F12+	6.70	6.82	5.95	7.52	7.04
VTZ-F12+	6.79	6.92	6.03	7.59	7.13
VQZ-F12+	6.81	6.94	6.05	7.59	7.16
			MRCI-F12+Q[a]		
VDZ-F12+	6.78	6.91	6.02	7.59	7.14
VTZ-F12+	6.82	6.96	6.06	7.57	7.22
VQZ-F12+	6.82	6.96	6.07	7.57	7.21

[a]The CABS singles corrections (CI) are included.

10. Representative numerical examples

In this section, we summarise some calculations presented in our earlier papers [33–35]. Fore more details and additional results, we refer to these papers. Since in Refs. [33, 34] the CABS singles correction was not yet available, the corresponding calculations have been repeated. Additional new calculations are presented for the potential curves of Cr_2 as well as for barrier heights and reaction energies of the $F + H_2 \rightarrow HF + H$ and $OH + CO \rightarrow CO_2 + H$ reactions.

10.1. Pyrrole excited states

The vertical excitation energies for low-lying states in the A_1 and B_2 symmetries of pyrrole (C_{2v} symmetry) have been computed by the SS CASPT2-F12 and MS MRCI-F12 methods with an active space of six electrons in four b_1 and three a_2 orbitals. The considered states have a Rydberg character except for the $\pi \rightarrow \pi^*$ valence state in the B_2 symmetry [39, 131]. Another valence state in the A_1 symmetry [39, 131] does not appear with this relatively small CAS. In order to describe the Rydberg states properly, the cc-pV*X*Z-F12 basis sets [132, 133] of C and N have been augmented by one even-tempered diffuse p function (see Ref. [33] for details). They are denoted by V*X*Z-F12+ in Table 4. Due to the more compact electronic structure of the ground state, dynamical electron correlation increases the excitation energies of the Rydberg states, and to recover this effect with conventional CASPT2 large basis sets are needed. At the double-ζ level, the standard CASPT2 method underestimates the excitation energies of the Rydberg states by 0.2–0.3 eV. In contrast, the CASPT-F12 method captures almost all of the basis-set error in the Rydberg excitation energies already with the double-ζ basis set, yielding a remarkably good accuracy of 0.03 eV (as compared to the CBS limit) for all states considered here. For the Rydberg excitations, the CASPT2 and MRCI+Q values are in rather good agreement, in most cases within 0.1–0.2 eV.

The basis-set convergence of the valence excitation energy in the B_2 symmetry is already good with the CASPT2 method and the F12 correction plays only a minor role. The accuracy of MRCI-F12+Q with double-ζ basis sets is 0.05 eV compared to the basis-set limit, while the basis-set truncation errors of the underlying MRCI+Q method is somewhat smaller than that of CASPT2. The CASPT2-F12 excitation energies for the B_2 valence excited state have a very large error of -1.24 eV relative to the corresponding MRCI-F12 values. As discussed previously [39], the CASPT2 valence excitation energies are often significantly underestimated, unless much larger active spaces are used. This observation is also confirmed by comparison with experimental excitation energies, although often basis-set and N-electron errors partly cancel.

10.2. CH_2 singlet–triplet separation

The singlet–triplet splitting in methylene is a long-standing problem in quantum chemistry since it strongly depends on basis-set and correlation effects. Table 5 demonstrates

Table 5. The singlet–triplet separation of CH_2 in kcal/mol. ΔE_S denotes the singles corrections to the energy differences. The geometries have been optimised for each method and basis set. Taken from Ref. [35].

OBS	CASSCF	CASPT2	CASPT2-F12	MRCI	MRCI-F12	MRCI-F12+ΔE_S
			CH_2 singlet–triplet splitting (full valence)			
VDZ-F12	10.58	14.19	13.02	10.12	9.29	8.78
VTZ-F12	10.12	13.44	12.73	9.01	8.57	8.53
VQZ-F12	10.11	13.16	12.75	8.73	8.51	8.50
CBS [56]		12.79		8.49		
			CH_2 singlet–triplet splitting [(7,4,3,1) orbitals]			
VDZ-F12	11.21	11.01	9.96	10.35	9.35	9.01
VTZ-F12	10.61	10.23	9.76	9.33	8.93	8.86
VQZ-F12	10.54	10.00	9.71	9.07	8.85	8.84
CBS [56]		9.72		8.83		

the effect of the F12 and singles corrections for the singlet–triplet splitting of CH_2 computed with SS CASPT2-F12 and MRCI-F12. Peterson's F12 orbital [132] and fitting [133] basis sets were used. Both the CASPT2-F12 and the MRCI-F12 methods capture most of the basis-set truncation errors in the correlation energy contributions already with small basis sets. The MRCI-F12 method combined with the singles correction reproduces the basis-set limit of the singlet–triplet splitting within 0.3 kcal/mol and 0.05 kcal/mol using the VDZ-F12 and VTZ-F12 basis sets, respectively. This is in contrast with the conventional MRCI, which was off by more than 1.5 kcal/mol with VDZ-F12. The singles corrections closely reproduce the basis-set truncation errors of CASSCF for both systems. Moreover, when the extended active space consisting of the full-valence + C(3*s*, 3*p*, 3*d*) orbitals is used, where the basis errors of CASSCF and the correlation energies of MRCI-F12 do not seem additive, the CABS singles corrected energies provide similar accuracy to that in the full-valence cases. The MRCI+F12 results obtained with this active space agree well with the experimental value of 9.1 $\pm$ 0.2 kcal/mol [134]. The latter value is corrected for the zero-point vibration energy and relativistic effects.

10.3. Cr dimer

The Cr dimer has been one of the most challenging systems for multireference electronic structure theories, and therefore there have been extensive studies in the past [18, 135–138]. One of the difficulties one encounters is that the binding energy is strongly dependent on the basis size [136], especially around the 3*d* bonding region. This is because *d* electrons already carry an angular momentum 2 and high-angular momentum basis functions are needed to describe the dynamical correlation effects.

In the current study, we have used the def2-QZVPP [139] orbital basis and the corresponding fitting basis sets [140] for the MRCI+Q and MRCI-F12+Q methods. The def2-QZVPP-jkfit fitting basis set contains up to *i* functions, and is able to fit products of three occupied *d* orbitals. This basis was also used for the CABS, which requires functions up to an angular momentum $3l_{\rm occ}$, i.e. in the current case up to $l = 6$ (*i* functions). In addition, a large orbital basis was used as a reference which consists of *s*,*p*,*d* shells of def2-QZVPP and even-tempered functions [(0.9, 2.2, 5), (0.9, 2.2, 5), (1.0, 2.2, 3), (1.1, 2.2, 2) for *f*, *g*, *h*, *i* shells, where these numbers stand for the centre and ratio of exponents and the number of even-tempered functions]. An active space with 12 electrons in 12 orbitals is used (correlating with the 3*d* and 4*s* atomic orbitals), which is a minimum choice for this system. All orbitals are optimised in the CASSCF step, while only 4*s* and 3*d* electrons are correlated in the MRCI; in other words, 3*s* and 3*p* electrons are treated as frozen cores in MRCI. Since they contribute significantly to the 3*d* bonding [136], we do not intend to compare our results with the experimental curve. Rather, we only intend to demonstrate the effect of the F12 terms on the potential energy curve.

As can be clearly seen from Figure 2, the 3*d* bonding is underestimated by around 0.2 eV when computed by the conventional MRCI+Q and def2-QZVPP basis sets. In contrast, the potential energy curve computed by the MRCI-F12+Q theory is even lower than the MRCI+Q one obtained with the large reference basis set. Likely, it is converged close to the basis-set limit. In order to achieve quantitative agreements with experiment, we plan to extend the F12 theory to the new MRCI with the Celani–Werner internal contraction recently studied by Shamasundar *et al.* [26], which is capable of correlating 3*s* and 3*p* electrons much more efficiently than our current program.

10.4. Excited states of ozone

The excited-state dynamics of ozone after photoexcitations of 1–6 eV are known to go through multiple conical intersections (see, for instance, Ref. [141], and references therein). Here we present the regions of the PESs around the conical intersections by MRCI+Q and MRCI-F12+Q

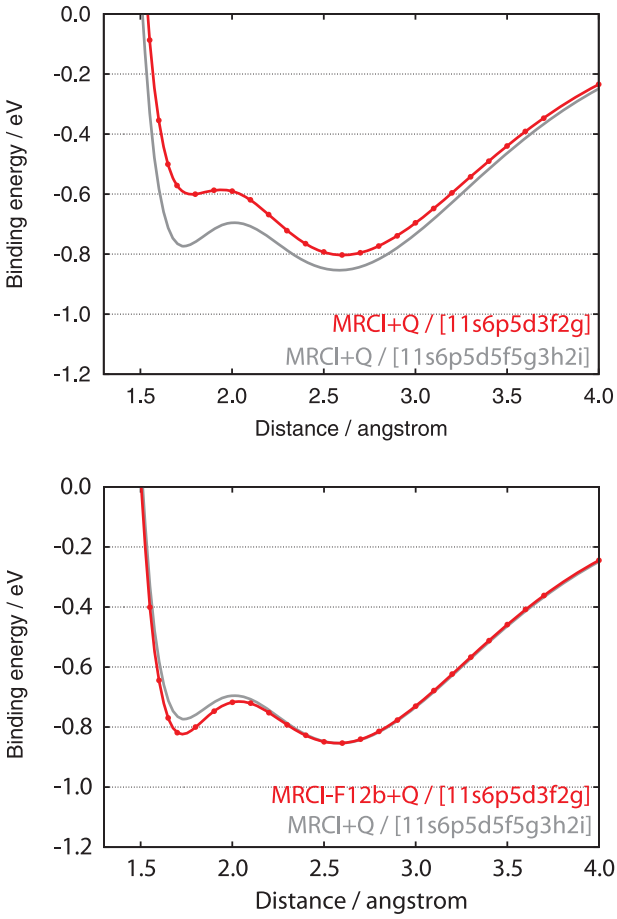

Figure 2. Cr dimer computed by MRCI+Q and MRCI-F12+Q. def2-QZVPP and extended basis functions were used for MRCI+Q, while MRCI-F12+Q was computed by def2-QZVPP. Note that 3*s* and 3*p* electrons were not correlated in this study.

calculations with various basis sets. We used the full-valence active space with frozen-core approximation. V*XZ*-F12 basis sets were used for the OBS and Weigend's auxiliary basis sets for DF and RI [142, 143]. The calculations were carried out in C_s symmetry, and five A' and six A'' states were averaged in the CASSCF, but only the five A' states have been calculated by MRCI and MRCI-F12. Figure 3 shows one-dimensional cuts of PESs as a function of the distance R_2, keeping $R_1 = 2.4$ bohr and $\angle_{OOO} = 116.8^\circ$ fixed. In addition, we show a two-dimensional cut with $\angle_{OOO} = 116.8^\circ$.

Although the vertical excitation energies from the equilibrium geometry of the ground state are quickly convergent to their complete basis-set limits with MRCI+Q, this is partly due to error cancellations between the basis-set truncation errors of the ground and excited states. However, the dissociation energies and the positions of the avoided crossings (associated with the conical intersections at C_{2v} geometries) are very sensitive to the size of the basis set. To achieve quantitative agreements with the conventional methods, one needs to use larger than the quadruple-ζ basis sets. MRCI-F12+Q remedies this problem to a large extent, and even the PESs computed with the double-ζ basis set are hardly distinguishable on the scale of the figure from those calculated with the quadruple-ζ basis set.

10.5. The F + H_2 reaction barrier height

MRCI methods are in most cases necessary to compute global PESs for chemical reactions. Prominent examples that have been studied extensively in the past are the F + $H_2 \rightarrow$ HF + H [144–147], Cl + $H_2 \rightarrow$ HCl + H [148–151] and OH + CO $\rightarrow$ CO_2 + H [152–156] reactions. Since at the transition states more electrons correlate with each other than in the reactants, the dynamical correlation effects

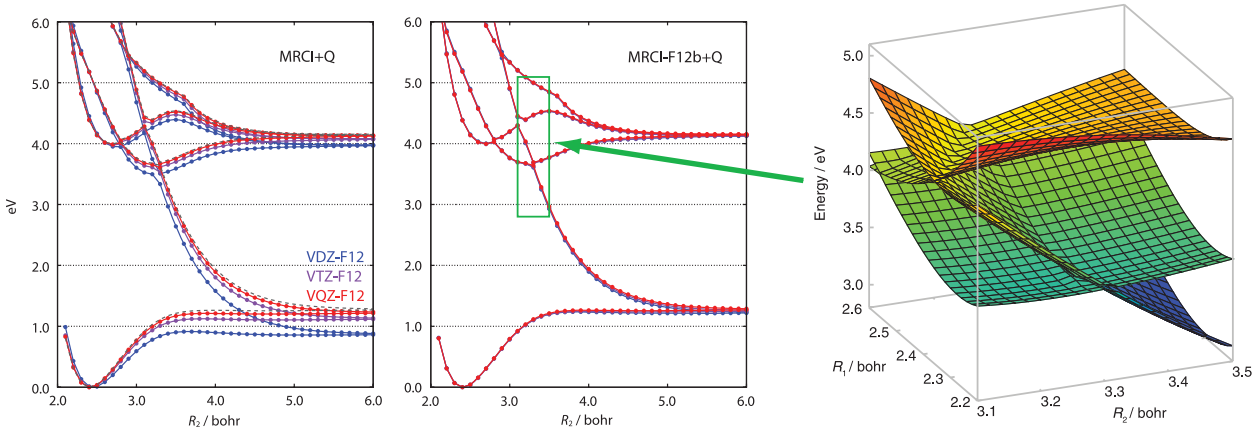

Figure 3. PESs of low-lying singlet A' states of ozone computed by MRCI+Q (left) and MRCI-F12b+Q (centre). One-dimensional cuts are made at one $R_1 = 2.4$ and $\angle_{OOO} = 116.8$. A two-dimensional cut with $2.2 \le R_1 \le 2.6$, $3.1 \le R_2 \le 3.5$ and $\angle_{OOO} = 116.8$ is also shown (MRCI-F12+Q and VDZ-F12), from which the fourth excited state was omitted for simplicity.

on the barrier heights are usually negative and very large. Furthermore, basis-set incompleteness effects can be large, and the resulting errors of the PESs may have a significant effect on the reaction dynamics.

A thorough study of basis-set and higher order correlation effects on the barrier and reaction energy of the F + H_2 reaction can be found in Ref. [127], and accurate global coupled MRCI+Q PESs for the three states that correlate with the F(^{2}P)+H_2 asymptote were presented in Ref. [144]. These results have been compared with MRCI-F12+Q calculations in Ref. [35]. Some results of this study for the bent transition state are shown in Table 6, along with additional calculations that include the CABS singles correction and the two coupled $^2A'$ states. The geometries are the same as in Refs. [35, 127]. For fluorine the aug-cc-pVXZ bases were used, while for the hydrogen atoms the non-augmented basis sets were used [this reduces basis-set superposition effects (BSSEs)]. This mixed basis will in the following be denoted by aVXZ.

MRCI-F12+Q with the aVQZ basis set is already converged to 0.01–0.02 kcal/mol as compared to the CBS limit. In contrast, the conventional MRCI+Q method requires the aug-cc-pV6Z basis set (or more) to achieve the same accuracy. In fact, the barriers obtained with MRCI+Q/aV6Z are still higher than those obtained with MRCI-F12+Q/aVQZ. One can observe that the CASSCF and correlation contributions have errors of different signs and partly cancel each other, unless the CABS singles correction is included. Most likely, the positive basis-set effect on the CASSCF barrier heights is due to BSSEs, which artificially lowers the CASSCF barrier if small basis sets are used; this effect decreases with increasing basis-set size. On the other hand, the negative effect of the dynamical correlation on the barrier heights strongly increases with increasing basis set size. Due to these compensating effects, the basis-set convergence of the MRCI-F12+Q method is somewhat deteriorated by the singles correction, since this eliminates the error compensation.

All MRCI and MRCI-F12 calculations in Table 6 include the Davidson correction, which has a large negative effect on the barrier height. As has been demonstrated and discussed in more detail in Ref. [127], it strongly matters how the Davidson correction is computed. It was found that best agreement with full-CI or coupled cluster with up to quadruple excitations (CCSDTQ) values is obtained by using the so-called Q1 version, in which the coefficient of the unrelaxed reference function in the final MRCI wavefunction is used to compute the correction (cf. Section 8.1).

In the MS calculations, the orbitals were optimised by state-averaged CASSCF including the three states (two $^2A'$, one $^2A''$) that are degenerate at the F(^2P) + H_2 asymptote. In the MS-MRCI calculations, the two $^2A'$ states were included. The Davidson correction was computed analogously to the Q1 correction, but using the rotated reference functions $|\tilde{M}\rangle$ that have best overlap with the final MRCI wavefunctions (cf. Equation 111). The two-state calculations yield a barrier height that is about 0.03 kcal/mol lower than obtained in the SS calculations. The final MS-MRCI-F12+Q value of 1.29 kcal/mol is still slightly higher than the CCSDTQ/CBS estimate of 1.20 kcal/mol [127]. Errors of this magnitude are within the uncertainty caused by the Davidson correction. For example, if the non-rotated reference function is used to compute the Davidson correction in the MS-MRCI case, the barrier is further reduced by ≈0.1 kcal/mol. In order to compare with experimental data, also core correlation, relativistic, non-Born–Oppenheimer and spin–orbit contributions must be included, which increase the barrier height by 0.442 kcal/mol [127].

10.6. The OH + CO reaction

As a final example we present some results for the OH + CO → CO_2 + H reaction, which involves a number of transition states and intermediates. Due to its importance in combustion processes, this reaction has been very extensively studied in the past, and various global PESs have been computed. For a review of earlier work, see Ref. [153]. Very recently, a new PES has been computed using CCSD(T)-F12b with the aug-cc-pVTZ basis set [154, 155, 156], and various quasi-classical dynamics studies have been reported in these and other papers [157, 158]. These and most older calculations of the PES used single-reference methods, which seem to work rather well even in the transition-state regions. However, the single-state treatments break down in some other regions of the PES, and therefore it is of interest to compare the single-reference CCSD(T)-F12b results with MRCI-F12 ones. To our knowledge, only one previous study used internally contracted MRCI wavefunctions [152].

We computed the relative energies of the transition states and intermediates in C_s symmetry with the CCSD(T)-F12b and MRCI-F12+Q methods, using the structures given in table 1 of Ref. [155]. For simplicity, we will omit in the following the +Q specification, with the understanding that Davidson's correction is always included. In contrast to the F + H_2 case, the various variants of the Davidson corrections give very similar results, and therefore the default Q0 method was used, in which the correction is computed using the coefficient of the relaxed reference function.

In the current study, the VXZ-F12 basis sets (X = D,T,Q) were employed, while Li *et al.* used the aug-cc-pVTZ basis. We also repeated the CCSD(T)-F12b calculations using the corresponding aug-cc-pVXZ basis sets (not shown here), and exactly reproduced the aug-cc-pVTZ results of Ref. [155]. Overall, both basis-set families yield results of comparable accuracy, although the convergence behaviour is somewhat different (for some structures, VXZ-F12 is slightly better, while for others, worse), which may be related to the more diffuse nature of the aug-cc-pVTZ basis, in particular for hydrogen.

Table 6. The bent reaction barrier of the F + H_2 reaction in kcal/mol. All MRCI and MRCI-F12 values have been corrected by Davidson's correction (see text).

OBS	CASSCF	SA-CASSCF	MRCI	MS-MRCI	MRCI -F12	MS-MRCI -F12	MRCI -F12+ΔE_S	MS-MRCI -F12+ΔE_S
aVTZ	7.304	7.589	1.795	1.766	1.333	1.350	1.451	1.354
aVQZ	7.427	7.712	1.433	1.401	1.294	1.280	1.338	1.288
aV5Z	7.475	7.760	1.386	1.353	1.310	1.287	1.316	1.288
aV6Z[a]	7.481	7.767	1.352	1.321				
CBS56	7.483	7.768	1.309	1.268				

[a]F12 calculations for the aV6Z basis were not performed since there are no fitting and CABS basis sets.

Table 7. MRCI-F12 calculations for various active spaces for the OH + CO → CO_2 + H reaction. Energies relative to trans-HOCO in kcal/mol, basis VTZ-F12. All valence orbitals are optimised and correlated; only the number of inactive orbitals has been varied. The active space is specified as electrons/orbital.

Method	OH + CO	cis-TS1	trans-TS1	cis-HOCO	cis-TS2	trans-TS4	HCOO(C_{2v})	TS3(C_{2v})	CO_2 + H
HF	3.860	20.701	12.887	0.040	43.642	52.867	39.326	28.793	−3.433
CASSCF(11/10)	0.119	16.302	8.658	0.331	29.423	46.180	12.607	22.414	1.472
CASSCF(13/11)	5.471	19.200	12.741	0.471	25.818	41.344	15.865	13.262	−14.561
CASSCF(17/13)	6.268	19.527	13.045	0.877	25.175	40.859	16.209	13.758	−13.887
MRCI-F12(11/10)	24.213	32.347	27.009	1.275	31.061	40.052	22.986	19.378	2.205
MRCI-F12(13/11)	25.418	31.483	27.248	1.342	31.091	38.959	16.434	18.967	1.041
MRCI-F12(17/13)	26.105	31.619	27.396	1.586	30.957	38.866	16.573	19.320	1.653
MRCI-F12+Q(11/10)	27.245	32.506	28.146	1.781	31.392	37.415	23.330	18.852	3.332
MRCI-F12+Q(13/11)	28.184	32.479	28.750	1.748	32.217	38.232	16.515	20.445	5.299
MRCI-F12+Q(17/13)	28.707	32.462	28.747	1.905	32.118	38.179	16.505	20.639	5.722
CCSD-F12b	26.123	31.494	27.166	1.622	34.872	41.052	20.884	23.606	7.686
CCSD(T)-F12b	29.202	32.427	28.735	1.803	31.923	38.365	16.710	20.802	6.803

Our results are presented in Tables 7 and 8. As in Ref. [155] all energies are in kcal/mol relative to the trans-HOCO intermediate, which is lowest in energy. In Table 7 the CASSCF and MRCI-F12 results for three different active spaces are compared to CCSD-F12 and CCSD(T)-F12 calculations, using the VTZ-F12 basis set. In all MRCI calculations, the full-valence orbital space was included, but the number of inactive orbitals in the reference function was three [active space: 11 electrons in 10 orbitals, denoted by (11/10)], two [active space (13/11)] or 0 [active space (17/13)]. It is found that the MRCI-F12 results in the latter two cases agree within a few tenths of a kcal/mol, while the (11/10) active space yields significantly larger errors. With increasing active space, the MRCI-F12 results systematically approach the CCSD(T)-F12b ones, and with the full-valence active space (17/13) the MRCI-F12 and CCSD(T)-F12b relative energies of all intermediate structures agree within about 0.2 kcal/mol. In view of the fact that the correlation effects are in many cases very large, this agreement is quite remarkable. The effect of the Davidson corrections on the relative energies typically amounts to 1–2 kcal/mol, and the (T) contributions are even larger. However, the energies of the asymptotic CO + OH and CO_2 + H energies relative to trans-HOCO show much larger deviations of 1.5 and 1.1 kcal/mol, respectively, between MRCI-F12 and CCSD(T)-F12b. Since all these structures are well described by single-reference wavefunctions, it is likely that the CCSD(T)-F12b results are most accurate. The large dynamical correlation effects (about 25 kcal/mol for OH+CO) are underestimated by the MRCI-F12 calculations. The reaction energies computed with the VTZ-F12 basis amount to −22.4 kcal/mol [CCSD(T)-F12b] and −23.0 kcal/mol (MRCI-F12). These values are changed to −22.6 and 23.2 kcal/mol, respectively, if the larger VQZ-F12 basis set is used (CCSD(T)-F12b/aug-cc-pV5Z yields −22.65 kcal/mol). The computed values bracket the experimental value of −22.8 kcal/mol (this is obtained from $\Delta H_r(0K) = -24.0$ kcal/mol and a zero-point correction of 1.20 kcal/mol).

The basis-set dependence of the MRCI and CCSD(T) results is compared in Table 8. Without the F12 treatment, the largest basis effects are found for the OH+CO asymptote and the trans-TS1 transition state, where the difference between the VDZ-F12 and VQZ-F12 MRCI values amounts to 5.4 and 4.5 kcal/mol, respectively. These effects are reduced to 0.81 and 0.69 kcal/mol, respectively, by inclusion of the F12 terms. The VTZ-F12 and VQZ-F12 values differ only by 0.1–0.2 kcal/mol. The convergence of the CCSD(T)-

Table 8. Basis-set dependence of relative energies for the OH + CO → CO_2 + H reaction. Energies relative to trans-HOCO in kcal/mol, basis VTZ-F12. All valence orbitals are optimised and correlated, active space (13/11); only the number of inactive orbitals has been varied. The active space is specified as electrons/orbital.

Method	Basis	OH + CO	cis-TS1	trans-TS1	cis-HOCO	cis-TS2	trans-TS4	HCOO(C_{2v})	TS3(C_{2v})	CO_2 + H
HF	VDZ-F12	2.846	19.802	11.986	−0.013	44.303	53.400	39.398	29.259	−2.745
HF	VTZ-F12	3.860	20.701	12.887	0.040	43.642	52.867	39.326	28.793	−3.433
HF	VQZ-F12	4.027	20.874	13.060	0.053	43.810	53.020	39.513	29.009	−3.144
CASSCF	VDZ-F12	4.261	18.379	11.935	0.407	26.243	41.637	15.792	13.502	−14.048
CASSCF	VTZ-F12	5.471	19.200	12.741	0.471	25.818	41.344	15.865	13.262	−14.561
CASSCF	VQZ-F12	5.634	19.353	12.894	0.478	25.988	41.489	16.035	13.466	−14.294
MRCI+Q	VDZ-F12	22.426	27.811	23.830	1.967	31.988	39.053	16.376	20.734	4.836
MRCI+Q	VTZ-F12	26.449	31.036	27.236	1.814	31.682	38.021	16.005	20.057	4.745
MRCI+Q	VQZ-F12	27.786	32.111	28.375	1.760	32.091	38.186	16.420	20.391	5.260
MRCI-F12+Q	VDZ-F12	27.642	32.066	28.287	1.754	32.349	38.435	16.680	20.683	5.367
MRCI-F12+Q	VTZ-F12	28.184	32.479	28.750	1.748	32.217	38.232	16.515	20.445	5.299
MRCI-F12+Q	VQZ-F12	28.453	32.688	28.972	1.735	32.266	38.306	16.617	20.492	5.339
CCSD(T)-F12b	VDZ-F12	28.468	31.894	28.165	1.841	31.782	38.395	16.670	20.890	6.558
CCSD(T)-F12b	VTZ-F12	29.202	32.427	28.735	1.803	31.923	38.365	16.710	20.802	6.803
CCSD(T)-F12b	VQZ-F12	29.482	32.599	28.931	1.788	31.975	38.405	16.817	20.848	6.881

F12b and MRCI-F12+Q values with increasing basis set is very similar.

A more thorough study of multireference and basis-set effects on the PES of this and other elementary reactions is in progress and will be presented elsewhere.

11. Conclusions

We have reviewed our recent developments in multireference explicitly correlated F12 theories. Their wavefunctions are transparent generalisations of the conventional WK internally contracted multireference wavefunctions. The same parametrisation is used to minimise the Hylleraas functional, the energy expectation value, and the ACPF functional to give the CASPT2-F12, MRCI-F12 and MRACPF-F12 methods. Some representative numerical results are shown to prove the significant acceleration of the basis-set convergence with the F12 theories. The additional cost caused by the F12 treatment is small as compared to the overall cost of MRCI calculations. Since the applicability of the MR-F12 methods is exactly the same as that of the underlying conventional MR methods, we believe that they can serve as powerful tools to tackle systems with complicated electronic structures in computational chemistry.

Acknowledgements

The authors thank Dr Kodagenahalli R. Shamasundar for a kind help on the Cr_2 calculations. This work has been supported by the Deutsche Forschungsgemeinschaft as part of an DFG-NSF project and by the Fonds der Chemischen Industrie. T.S. is supported by the Japan Society for the Promotion of Science Research Fellowship for Research Abroad.

References

[1] R.J. Bartlett and M. Musiał, Rev. Mod. Phys. **79**, 291 (2007).
[2] M.E. Harding, J. Vázquez, B. Ruscic, A.K. Wilson, J. Gauss and J.F. Stanton, J. Chem. Phys. **128**, 114111 (2008).
[3] H. Lischka, R. Shepard, F.B. Brown and I. Shavitt, Int. J. Quantum Chem., Quantum Chem. Symp. **15**, 91 (1981).
[4] K. Hirao, Chem. Phys. Lett. **190**, 374 (1992).
[5] H. Nakano, J. Chem. Phys. **99**, 7983 (1993).
[6] U.S. Mahapatra, B. Datta and D. Mukherjee, J. Chem. Phys. **110**, 6171 (1999).
[7] F.A. Evangelista, W.D. Allen and H.F. Schaefer , J. Chem. Phys. **127**, 024102 (2007).
[8] W. Meyer, in *Modern Theoretical Chemistry*, edited by H.F. Schaefer (Plenum, New York, 1977), Vol. 3, Chap. 11.
[9] P.E.M. Siegbahn, Int. J. Quant. Chem. **1**, 1229 (1980).
[10] H.-J. Werner and E.A. Reinsch, J. Chem. Phys. **76**, 3144 (1982).
[11] B.O. Roos, P. Linse, P.E.M. Siegbahn and M.R.A. Blomberg, Chem. Phys. **66**, 197 (1981).
[12] K. Andersson, P.-Å. Malmqvist, B.O. Roos, A.J. Sadlej and K. Wolinski, J. Phys. Chem. **94**, 5483 (1990).
[13] K. Andersson, P.-Å. Malmqvist and B.O. Roos, J. Chem. Phys. **96**, 1218 (1992).
[14] H.-J. Werner, Mol. Phys. **89**, 645 (1996).
[15] J. Finley, P.-Å. Malmqvist, B.O. Roos and L. Serrano-Andrés, Chem. Phys. Lett. **288**, 299 (1988).
[16] P. Celani and H.-J. Werner, J. Chem. Phys. **112**, 5546 (2000).
[17] F. Aquilante, P.-Å. Malmqvist, T.B. Pedersen, A. Ghosh and B.O. Roos, J. Chem. Theory Comput. **4**, 694 (2008).
[18] Y. Kurashige and T. Yanai, J. Chem. Phys. **135**, 094104 (2011).
[19] C. Angeli, R. Cimiraglia, S. Evangelisti, T. Leininger and J.P. Malrieu, J. Chem. Phys. **114**, 10252 (2001).
[20] C. Angeli, R. Cimiraglia and J.P. Malrieu, J. Chem. Phys. **117**, 9138 (2002).
[21] C. Angeli, M. Pastore and R. Cimiraglia, Theor. Chem. Acc. **117**, 743 (2007).

[22] H.-J. Werner and E.A. Reinsch, in Proceedings of the Fifth Seminar on Computational Methods in Quantum Chemistry, edited by T.H. van Duinen and W.C. Niewpoort (Max-Planck Institut Garching, München, 1981).
[23] H.-J. Werner and E.A. Reinsch, in Advanced Theories and Computational Approaches to the Electronic Structure of Molecules, edited by C.E. Dykstra, Vol. **133** (D. Reidel, Dordrecht, 1984).
[24] H.-J. Werner and P.J. Knowles, J. Chem. Phys. **89**, 5803 (1988).
[25] P.J. Knowles and H.-J. Werner, Chem. Phys. Lett. **145**, 514 (1988).
[26] K.R. Shamasundar, G. Knizia and H.-J. Werner, J. Chem. Phys. **135**, 054101 (2011).
[27] T. Yanai and G.K.-L. Chan, J. Chem. Phys. **124**, 194106 (2006).
[28] E. Neuscamman, T. Yanai and G.K.-L. Chan, Int. Rev. Phys. Chem. **29**, 231 (2010).
[29] T. Yanai, Y. Kurashige, E. Neuscamman and G.K.-L. Chan, J. Chem. Phys. **132**, 024105 (2010).
[30] F.A. Evangelista and J. Gauss, J. Chem. Phys. **134**, 114102 (2011).
[31] M. Hanauer and A. Köhn, J. Chem. Phys. **134**, 204111 (2011).
[32] F. Aquilante, T.B. Pedersen, R. Lindh, B.O. Roos, A. Sánchez de Merás and H. Koch, J. Chem. Phys. **129**, 024113 (2008).
[33] T. Shiozaki and H.-J. Werner, J. Chem. Phys. **133**, 141103 (2010).
[34] T. Shiozaki, G. Knizia and H.-J. Werner, J. Chem. Phys. **134**, 034113 (2011).
[35] T. Shiozaki and H.-J. Werner, J. Chem. Phys. **134**, 184104 (2011).
[36] T. Shiozaki, W. Győrffy, P. Celani and H.-J. Werner, J. Chem. Phys. **135**, 081106 (2011).
[37] T. Shiozaki, C. Woywod and H.-J. Werner, Phys. Chem. Chem. Phys. **15**, 262 (2013).
[38] A.A. Granovsky, J. Chem. Phys. **134**, 214113 (2011).
[39] P. Celani and H.-J. Werner, J. Chem. Phys. **119**, 5044 (2003).
[40] W. Győrffy, T. Shiozaki, G. Knizia and H.-J. Werner, J. Chem. Phys. **138**, 104104 (2013).
[41] W. Kutzelnigg, Theor. Chim. Acta **68**, 445 (1985).
[42] W. Klopper and W. Kutzelnigg, Chem. Phys. Lett. **134**, 17 (1987).
[43] W. Kutzelnigg and W. Klopper, J. Chem. Phys. **94**, 1985 (1991).
[44] S. Ten-no, Chem. Phys. Lett. **398**, 56 (2004).
[45] S. Ten-no, J. Chem. Phys. **126**, 014108 (2007).
[46] R.J. Gdanitz, Chem. Phys. Lett. **210**, 253 (1993).
[47] R.J. Gdanitz, Chem. Phys. Lett. **283**, 253 (1998).
[48] S. Ten-no, Chem. Phys. Lett. **447**, 175 (2007).
[49] M. Torheyden and E.F. Valeev, J. Chem. Phys. **131**, 171103 (2009).
[50] S. Kedžuch, O. Demel, J. Pittner, S. Ten-no and J. Noga, Chem. Phys. Lett. **511**, 418 (2011).
[51] L. Kong and E.F. Valeev, J. Chem. Phys. **135**, 214105 (2011).
[52] R. Haunschild, S. Mao, D. Mukherjee and W. Klopper, Chem. Phys. Lett. **531**, 247 (2012).
[53] H.-J. Werner, P.J. Knowles, G. Knizia, F.R. Manby and M. Schütz, WIRES Comput. Mol. Sci. **2**, 242 (2012).
[54] P.J. Knowles and H.-J. Werner, Theor. Chim. Acta **84**, 95 (1992).
[55] T. Shiozaki, C. Woywod and H.-J. Werner, Phys. Chem. Chem. Phys. **15**, 262 (2013).
[56] H.-J. Werner, T.B. Adler, G. Knizia and F.R. Manby, in Recent Progress in Coupled Cluster Methods, edited by P. Cársky, J. Paldus and J. Pittner (Springer, Berlin, 2010).
[57] D.P. Tew, C. Hättig, R.A. Bachorz and W. Klopper, in Recent Progress in Coupled Cluster Methods, edited by P. Cársky, J. Paldus and J. Pittner (Springer, Berlin, 2010).
[58] C. Hättig, W. Klopper, A. Köhn and D.P. Tew, Chem. Rev. **112**, 4 (2012).
[59] L. Kong, F.A. Bischoff and E.F. Valeev, Chem. Rev. **112**, 75 (2012).
[60] E.A. Hylleraas, Z. Phys. **54**, 347 (1929).
[61] T. Kato, Commun. Pure. Appl. Math. **10**, 151 (1957).
[62] R.T. Pack and W. Byers Brown, J. Chem. Phys. **45**, 556 (1966).
[63] S.F. Boys and N.C. Handy, Proc. Roy. Soc. London Ser. A. **309**, 209 (1969).
[64] S. Ten-no, Chem. Phys. Lett. **330**, 169 (2000).
[65] H. Luo, J. Chem. Phys. **133**, 154109 (2010).
[66] K. Szalewicz, B. Jeziorski, H.J. Monkhorst and J.G. Zabolitzky, Chem. Phys. Lett. **91**, 169 (1982).
[67] B. Jeziorski, H.J. Monkhorst, K. Szalewicz and J.G. Zabolitzky, J. Chem. Phys. **81**, 368 (1984).
[68] K. Szalewicz, W. Kołos, H.J. Monkhorst and C. Jackson, J. Chem. Phys. **81**, 2723 (1984).
[69] J. Rychlewski, editor, *Explicitly Correlated Wave Functions in Chemistry and Physics* (Kluwer Academic Publishers, Dordrecht, 2003).
[70] W. Klopper, F.R. Manby, S. Ten-no and E.F. Valeev, Int. Rev. Phys. Chem. **25**, 427 (2006).
[71] W. Klopper, Chem. Phys. Lett. **186**, 583 (1991).
[72] J. Noga, W. Kutzelnigg and W. Klopper, Chem. Phys. Lett. **199**, 497 (1992).
[73] J. Noga and W. Kutzelnigg, J. Chem. Phys. **101**, 7738 (1994).
[74] MOLPRO, version 2006.1, a package of ab initio programs, H.-J. Werner, P. J. Knowles, R. Lindh, F. R. Manby, M. Schäutz, P. Celani, T. Korona, G. Rauhut, R. D. Amos, A. Bernhardsson, A. Berning, D. L. Cooper, M. J. O. Deegan, A. J. Dobbyn, F. Eckert, C. Hampel and G. Hetzer, A.W. Lloyd, S. J. McNicholas,W. Meyer and M. E. Mura, A. Nicklass, P. Palmieri, R. Pitzer, U. Schumann, H. Stoll, A. J. Stone, R. Tarroni and T. Thorsteinsson, see http://www.molpro.net.
[75] Turbomole V6.3 2011, a development of University of Karlsruhe and Forschungszentrum Karlsruhe GmbH, 1989–2007, TURBOMOLE GmbH, since 2007; available from `http://www.turbomole.com`.
[76] C.L. Janssen, I.B. Nielsen, M.L. Leininger, E.F. Valeev and E.T. Seidl, *MPQC, the Massively Parallel Quantum Chemistry Program*, Version 3.0.0α (Sandia National Laboratories, Livermore, CA, 2006).
[77] *GELLAN*: *A Hierarchical Quantum Chemistry Program* (Kobe University, Kobe, Japan, 2010).
[78] W. Klopper and C.C.M. Samson, J. Chem. Phys. **116**, 6397 (2002).
[79] E.F. Valeev, Chem. Phys. Lett. **395**, 190 (2004).
[80] D.P. Tew and W. Klopper, J. Chem. Phys. **125**, 094302 (2006).
[81] H.-J. Werner, T.B. Adler and F.R. Manby, J. Chem. Phys. **126**, 164102 (2007).
[82] K.A. Peterson, C. Krause, H. Stoll, J.G. Hill and H.-J. Werner, Mol. Phys. **109**, 2607 (2011).
[83] F.R. Manby, J. Chem. Phys. **119**, 4607 (2003).
[84] S. Ten-no and F.R. Manby, J. Chem. Phys. **119**, 5358 (2003).

[85] S. Kedžuch, M. Milko and J. Noga, Int. J. Quantum Chem. **105**, 929 (2005).
[86] T.B. Adler, G. Knizia and H.-J. Werner, J. Chem. Phys. **127**, 221106 (2007).
[87] G. Knizia and H.-J. Werner, J. Chem. Phys. **128**, 154103 (2008).
[88] J. Noga and J. Šimunek, Chem. Phys. **356**, 1 (2008).
[89] L. Kong and E.F. Valeev, J. Chem. Phys. **133**, 174126 (2010).
[90] T. Shiozaki, M. Kamiya, S. Hirata and E.F. Valeev, Phys. Chem. Chem. Phys. **10**, 3358 (2008).
[91] T. Shiozaki, M. Kamiya, S. Hirata and E.F. Valeev, J. Chem. Phys. **129**, 071101 (2008).
[92] A. Köhn, G.W. Richings and D.P. Tew, J. Chem. Phys. **129**, 201103 (2008).
[93] T. Shiozaki, M. Kamiya, S. Hirata and E.F. Valeev, J. Chem. Phys. **130**, 054101 (2009).
[94] H.-J. Werner, J. Chem. Phys. **129**, 101103 (2008).
[95] T.B. Adler, H.-J. Werner and F.R. Manby, J. Chem. Phys. **130**, 054106 (2009).
[96] T.B. Adler and H.-J. Werner, J. Chem. Phys. **130**, 241101 (2009).
[97] D.P. Tew, B. Helmich and C. Hättig, J. Chem. Phys. **135**, 074107 (2011).
[98] T.B. Adler and H.-J. Werner, J. Chem. Phys. **135**, 144117 (2011).
[99] T. Shiozaki and S. Hirata, J. Chem. Phys. **132**, 151101 (2010).
[100] F.A. Bischoff, S. Höfener, A. Glöß and W. Klopper, Theor. Chem. Acc. **121**, 11 (2008).
[101] F.A. Bischoff and W. Klopper, J. Chem. Phys. **132**, 094108 (2010).
[102] F.A. Bischoff, E.F. Valeev, W. Klopper and C.L. Janssen, J. Chem. Phys. **132**, 214104 (2010).
[103] Z. Li, S. Shao and W. Liu, J. Chem. Phys. **136**, 144117 (2012).
[104] S. Ten-no and D. Yamaki, J. Chem. Phys. **137**, 131101 (2012).
[105] C. Neiss and C. Hättig, J. Chem. Phys. **126**, 154101 (2005).
[106] C. Neiss, C. Hättig and W. Klopper, J. Chem. Phys. **125**, 064111 (2006).
[107] A. Köhn, J. Chem. Phys. **130**, 104104 (2009).
[108] M. Hanauer and A. Köhn, J. Chem. Phys. **131**, 124118 (2009).
[109] J. Yang and C. Hättig, J. Chem. Phys. **131**, 074102 (2009).
[110] A. Köhn, J. Chem. Phys. **130**, 131101 (2009).
[111] A. Köhn, J. Chem. Phys. **133**, 174118 (2010).
[112] H. Fliegl, W. Klopper and C. Hättig, J. Chem. Phys. **122**, 084107 (2005).
[113] H. Fliegl, C. Hättig and W. Klopper, Int. J. Quantum Chem. **106**, 2306 (2006).
[114] D.P. Tew, W. Klopper and C. Hättig, Chem. Phys. Lett. **452**, 326 (2008).
[115] H.-J. Werner, G. Knizia and F.R. Manby, Mol. Phys. **109**, 407 (2011).
[116] E.F. Valeev, Phys. Chem. Chem. Phys. **10**, 108 (2008).
[117] M. Torheyden and E.F. Valeev, Phys. Chem. Chem. Phys. **10**, 3410 (2008).
[118] E.F. Valeev and T.D. Crawford, J. Chem. Phys. **128**, 244113 (2008).
[119] C. Hättig, D.P. Tew and A. Köhn, J. Chem. Phys. **132**, 231102 (2010).
[120] S.A. Varganov and T.J. Martínez, J. Chem. Phys. **132**, 054103 (2010).
[121] W. Kutzelnigg and D. Mukherjee, J. Chem. Phys. **107**, 432 (1997).
[122] Y. Ohtsuka and S. Nagase, Chem. Phys. Lett. **463**, 431 (2008).
[123] G.H. Booth, A.J.W. Thom and A. Alavi, J. Chem. Phys. **131**, 054106 (2009).
[124] K.G. Dyall, J. Chem. Phys. **102**, 4909 (1995).
[125] G. Knizia, T.B. Adler and H.-J. Werner, J. Chem. Phys. **130**, 054104 (2009).
[126] E.R. Davidson and D.W. Silver, Chem. Phys. Lett. **53**, 403 (1977).
[127] H.-J. Werner, M. Kállay and J. Gauss, J. Chem. Phys. **128**, 034305 (2008).
[128] R.J. Gdanitz and R. Ahlrichs, Chem. Phys. Lett. **143**, 413 (1988).
[129] P.G. Szalay and R.J. Bartlett, Chem. Phys. Lett. **214**, 481 (1993).
[130] K.E. Yousaf and K.A. Peterson, Chem. Phys. Lett. **476**, 303 (2009).
[131] B.O. Roos, P.-Å. Malmqvist, V. Molina, L. Serrano-Andrés and M. Merchán, J. Chem. Phys. **116**, 7526 (2002).
[132] K.A. Peterson, T.B. Adler and H.-J. Werner, J. Chem. Phys. **128**, 084102 (2008).
[133] K.E. Yousaf and K.A. Peterson, J. Chem. Phys. **129**, 184108 (2008).
[134] I. Shavitt, Tetrahedron **41**, 1531 (1985).
[135] B.O. Roos and K. Andersson, Chem. Phys. Lett. **245**, 215 (1995).
[136] P. Celani, H. Stoll, H.-J. Werner and P.J. Knowles, Mol. Phys. **21**, 2369 (2004).
[137] C. Angeli, B. Bories, A. Cavallini and R. Cimiraglia, J. Chem. Phys. **124**, 054108 (2006).
[138] T. Müller, J. Phys. Chem. A **113**, 12729 (2009).
[139] F. Weigend, F. Furche and R. Ahlrichs, J. Chem. Phys **119**, 12753 (2003).
[140] C. Hättig, Phys. Chem. Chem. Phys. **7**, 59 (2005).
[141] S.Y. Grebenshchikov, Z.W. Qu, H. Zhu and R. Schinke, Phys. Chem. Chem. Phys. **9**, 2044 (2007).
[142] F. Weigend, A. Köhn and C. Hättig, J. Chem. Phys. **116**, 3175 (2002).
[143] F. Weigend, Phys. Chem. Chem. Phys. **4**, 4285 (2002).
[144] G. Li, H.-J. Werner, F. Lique and M.H. Alexander, J. Chem. Phys. **127**, 174302 (2007).
[145] L. Che, Z. Ren, X. Wang, W. Dong, D. Dai, X. Wang, D.H. Zhang, X. Yang, L. Sheng, G. Li, H.-J. Werner, F. Lique and M.H. Alexander, Science **317**, 1061 (2007).
[146] F. Lique, M.H. Alexander, G. Li, H.-J. Werner, S.A. Nizkorodov, W.W. Harper and D.J. Nesbitt, J. Chem. Phys. **128**, 084313 (2008).
[147] F. Lique, G. Li, H.-J. Werner and M.H. Alexander, J. Chem. Phys. **134**, 231101 (2011).
[148] W. Bian and H.-J. Werner, J. Chem. Phys. **112**, 220 (2000).
[149] M.H. Alexander, G. Capecchi and H.-J. Werner, Science **296**, 715 (2002).
[150] G. Capecchi and H.-J. Werner, Phys. Chem. Chem. Phys. **6**, 4975 (2004).
[151] X. Wang, W. Dong, C. Xiao, L. Che, Z. Ren, D. Dai, X. Wang, P. Casavecchia, X. Yang, B. Jiang, D. Xie, Z. Sun, S.Y. Lee, D.H. Zhang, H.-J. Werner and M.H. Alexander, Science **322**, 573 (2008).
[152] X. Song, J. Li, H. Hou and B. Wang, J. Chem. Phys. **125** (9), 094301 (2006).
[153] J.S. Francisco, J.T. Muckerman and H.G. Yu, Acc. Chem. Res. **43** (12), 1519 (2010).

[154] J. Li, Y. Wang, B. Jiang, J. Ma, R. Dawes, D. Xie, J.M. Bowman and H. Guo, J. Chem. Phys. **136** (4), 041103 (2012).
[155] J. Li, C. Xie, J. Ma, Y. Wang, R. Dawes, D. Xie, J.M. Bowman and H. Guo, J. Phys. Chem. A **116** (21), 5057 (2012).
[156] C. Xie, J. Li, D. Xie and H. Guo, J. Chem. Phys. **137** (2), 024308 (2012).
[157] E. García, J.C. Corchado and J. Espinosa-García, Comput. Theor. Chem. **990**, 47 (2012).
[158] J. Ma, J. Li and H. Guo, Phys. Rev. Lett. **109**, 063202 (2012).